UCLouvain

École polytechnique de Louvain

# Optimization of the Seine Aval wastewater treatment plant

Author: **Tom De Beugher**
Supervisor: **Denis Dochain**
Readers: **Denis Dochain, Francesco Contino, Raphaël Jungers**
Academic year 2021–2022
Master [120] in Mechanical Engineering

# Contents

# Abstract

The Seine-Aval wastewater treatment plant treats daily 1,600,000 $m^3$ of wastewater discharged into the Seine. Its performance therefore has a major environmental impact.

In this thesis, a simplified model derived from activated sludge models (ASM) is implemented in Simulink to represent the different units of the WasteWater Treatment Plant (WWTP). This model has been calibrated on the available data.

It then performs an optimization of the flows between the units of the station for three typical exploitation's conditions. This optimization uses as an objective function the Effluent Quality Index (EQI). The Genetic Algorithm (GA) and Sequential Quadratic Programming (SQP) method are tested to perform this optimization.

The optimizations expose good results in a reasonable amount of time.

# Acknowledgment

I would like to thank Denis Dochain for his advice and his availability during this year. I would also like to thank my mother for her support during the writing of this thesis. Finally, I cannot fail to thank my best friend Jimmy for his support, his intensive proofreading and his numerous advices.

# Introduction

### Context

In recent years, environmental protection has become a major concern in Europe [1]. In this context, the European community (EC) has set ambitious objectives and precise legal framework for wastewater management. This was firstly done through a Urban Waste Water Treatment Directive (UWWTD) in 1991[2]. This directive aims to protect the environment and human health from the adverse effects of urban wastewater discharges. It focuses on the collection, the treatment and the discharge of the wastewater coming from domestic and industrial sectors.

The evaluation of the UWWTD in 2019 demonstrated the Directive's effectiveness to reduce pollution coming from urban sources [3]. It also identified a number of issues. It notably reported the lack of effective management of some treatment plants and the ability of the plants to handle large flows during heavy rainfall. This is why the directive is currently in the process of being amended [4].

In Paris, the Seine-Aval WasteWater Treatment Plant (WWTP) is the largest in Europe. It covers 800 ha and treats daily an average of $1,6 \cdot 10^6$ $m^3$ of wastewater. This is equivalent to the wastewater production of 70 % of the population of Paris.

One of the major concern of such a plant is to maintain the same treatment quality regardless of the weather. Indeed, meteorological conditions induce strong variations of the flow and composition of the wastewater.

To improve the management of the station, the "Syndicat interdépartemental pour l'assainissement" SIAAP (Interdepartmental Syndicate for Sanitation) launch in 2014 the research program "MOdélisation, Contrôle et Optimisation des Procédés d'Epuration des Eaux", MOCOPEE (Modeling, Control and Optimization of Water Treatment Processes). It is a permanent working and exchange space between scientists and operational actors of wastewater treatment. The program deals with issues related to the metrology, the modelling and the control of treatment processes. It also deals with some emergent innovative concepts in the field of sanitation.

### Proposed work

This master thesis tackles the modelling and optimisation of the complex Seine-Aval wastewater treatment plant. Indeed, due to advances in understanding, control and modelling, the complexity of the system keeps increasing. More than a description of the existing models, this thesis takes up the challenge to test new methods to optimize the control.

For wastewater treatment plants, it can be advantageous to use predictive control, i.e. control that optimises commands based on anticipations of the system dynamics.

Ben Ayed et al. already investigated a method of predictive control requiring linearization of the system [5]. This work tests optimization methods that do not require linearization of the model. This approach allows to take into account the change of the system dynamics due to the variations of the operating conditions.

### Work structure

To explain the whole approach, the text is divided into three chapters :

**Chapter 1 - State of the Art :** It first synthesizes the knowledge concerning wastewater composition and then describes the working of wastewater treatment plants. Then, it details the Seine-Aval wastewater treatment plant and the models used to simulate it. Finally, a synthesis of the optimization methods that can be used in this work is given.

**Chapter 2 - Model Implementation :** The second part of this thesis focuses on the implementation of the model presented in the previous section. This part will be decomposed as follows : A presentation of the program used, then a calibration and test of the program for each section of the treatment plant.

**Chapter 3 - Optimization :** In the last part, the chosen model is used to test different optimization methods for three typical days (dry day,rainy day and heavy rain). It details how the flow between the different parts of the plant is enhanced.

# Chapter 1

# State of the Art

## Introduction

In this chapter the theoretical and contextual basis for the rest of the work is given. It starts by informing the reader about the basic information concerning wastewater treatment. Then the Seine-Aval plant and the models used to simulate it are presented. Finally, optimisation algorithms are introduced.

## 1.1 Wastewater treatment

This first section begins with an explanation of the composition of wastewater and the adverse effects that some of its constituents may have on the environment. Next, the water framework directive is explained. Finally, an in-depth look at the different types of wastewater treatment is given.

### 1.1.1 Wastewater composition, measurement and origins

#### Wastewater compostion

The generation of garbage as a result of human activity is inescapable. A lot of human waste ends up as wastewater. The quantity and composition of wastewater can vary a lot depending on location and time. Several factors play a role in this variation. For instance, the water consumption of the population, the weather, the sewage system... In this section a overview of the wastewater composition is given. Wastewater sources are mainly divided into two categories. The first one is call domestic wastewater, i.e. wastewater from homes. The second is industrial wastewater, which is mainly treated in a specific way by the industries.

The main components found in wastewater and their adverse effects are presented in the following Table 1.1.

| Wastewater constituents | | Effects |
|---|---|---|
| Microorganisms | Pathogenic bacteria, virus and worms eggs | Risk when bathing and eating shellfish |
| Biodegradable organic materials | Oxygen depletion | Fish death, odours |
| Other organic materials | Detergents, pesticides, fat, oil and grease, colouring, solvents, phenols, cyanide | Toxic effect, aesthetic inconveniences, bio accumulation in the food chain |
| Nutrients | Nitrogen, phosphorus | Eutrophication, oxygen depletion, toxic effect |
| Metals | Hg, Pb, Cd, Cr, Cu, Ni | Toxic effect, bioaccumulation |
| Other inorganic materials | Acids, for example hydrogen sulphide, bases | Corrosion, toxic effect |

Table 1.1: Main wastewater constituent and her adverse effects, adapted from [6]

### Wastewater measurement

Measurement are based on the concentrations of the following components:

- **Organic matter**, that are measured either by the Chemical Oxygen Demand (COD) or by the Biological Oxygen Demand (BOD) of the system. It should be noted that the COD is quicker than BOD to measure but can be polluting when mercury is used. The measurement of BOD is very slow (up to 5 days).
- In **nutrients**, there are organic matter composed of nitrogen as well as nitrites ($NO_2^-$), nitrates ($NO_3^-$) and ammonium ($NH_4^+$). The compounds containing phosphorus are also classified in the nutrients, we find mainly ortho-phosphates ($PO_4^{3-}$).
- **Total Suspended Solids (TSS)** are all particles of minerals, sand, sludge, organic matter (including microorganisms) or other matter between $1\mu m$ and 1mm that are not dissolved .

### Wastewater origins

Domestic wastewater accounts for 85 % of the volume of water treated by the Seine-Aval plant, while industrial wastewater accounts for 5 % [7]. Details of the composition of domestic wastewater according to a European study [8] are given in the Table 1.2.

| Parameters | **Collected data** | | | | | | **Reference** | **Unit** |
|---|---|---|---|---|---|---|---|---|
| | Sewage | | | Greywater | | E.U. domestics | | |
| | Urine hydrolyzed | Fecal matter | Toilet paper | Personal hygiene | Food and cleaning | Contributions sum | Domestic wastewater | |
| **Volume** | | | | | | | | |
| without flush | 1.3 | 0.1 | 0.0 | 39.0 | 44.0 | 84.4 | | $L.pers^{-1}.j^{-1}$ |
| with flush | | 36.0 | | 39.0 | 44.0 | 119.0 | | |
| Flush volume according to equipment | | 6-73 | | | | 89-156 | | |
| **TSS** | 1 | 26 | 23 | 3 | 15 | 67 | **72** | |
| **BOD** | 5 | 23 | 12 | 5 | 21 | 65 | 60 | $g.pers^{-1}.j^{-1}$ |
| **COD** | 9 | 37 | 27 | 8 | 52 | 133 | **156** | |
| **NGL** | 7.7 | 1.6 | 0.0 | 0.3 | 0.8 | 10.4 | **15** | |
| **PT** | 0.6 | 0.8 | 0.0 | 0.0 | 1.2 | 2.6 | 2 | $g.pers^{-1}.j^{-1}$ |
| - $P\text{-}PO_4$ | 0.7 | 0.4 | 0.0 | 0.1 | 0.6 | 1.7 | | |

Table 1.2: Composition of domestic wastewater by emission source at the household level, adapted from [8]

The Table 1.2 shows that the amount of wastewater produced in everyday life is equally divided between flushing, personal hygiene, cleaning and food. In this study, the amount of water produced per person is on average 119 liter per person and per day.

The contribution of organic matter and TSS is mainly due to faeces and toilet paper. A contribution from food and cleaning activities is not negligible either. Concerning the nutrients, they are mainly found in the urine for nitrogen and in the water from washing machines, faeces and urine for phosphorus.

### 1.1.2 Water framework directive

Wastewater treatment is subject to a European regulation (the UWWTD directive [2] as explained in the introduction). This directive imposes different maximum values of concentrations at the outlet of the wastewater treatment plant and/or a minimum percentage of decrease of this concentration (see table 1.3 and table 1.4). These values are defined according to the size of the treatment plant. Each year, a minimum number of samples must be taken by the treatment plant.

The wastewater leaving the plant is considered to be in compliance if:

- The maximum number of samples not complying with the limits (see the Table 1.3 for the limits definition) does not exceed a fixed value (see [9] for the maximum number of samples)
- No daily concentration exceeds 100% (150% for TSS) of the fixed limit given in Table 1.3
- The annual average concentration does not exceed a limit (see Table 1.4)

Note that some exceptions are provided in the directive, e.g. in case of storms. For more information the reader is invited to consult the directive [2], and the french legal framework [9]. Note also that the directive of 1991 [2] was clarified by a new directive in 1998 [10].

| Parameters | Limit | Minimal reduction | Redhibitory values | Units |
|---|---|---|---|---|
| BOD | 25 | 70-90 % | 50 | $g_{O_2}/m^3$ |
| COD | 125 | 75% | 250 | $g_{O_2}/m^3$ |
| TSS | 35 | 90 % | 85 | $gm^3$ |

Table 1.3: Requirements for discharges from urban waste water treatment plants subject to the provisions of Articles 4 and 5 of the directive

| Parameters | Limit | Minimal reduction | Units |
|---|---|---|---|
| P total | 1 | 80 % | $g_P/m^3$ |
| N total | 10 | 70 % | $g_N/m^3$ |

Table 1.4: Requirements for discharges from urban waste water treatment plants in sensitive areas subject to eutrophication

### 1.1.3 Treatment

Wastewater is usually treated in four steps: the pre-treatment, the primary, the secondary and the tertiary treatment. [11, 12].

#### Pre-treatment

The objective of pre-treatment is to prevent undesirable elements (coarse solids, sand oil, etc.) from going in the upstream installations. Indeed, sand wears out the infrastructure by abrasion and can cause the clogging of pipes. Oil products foam in the aeration installations and reduces the biological treatments performances.

The treatment consists in a grid filter for the big waste, a desander and a de-oiler that collects mechanically the oils on the surface. There are also station-specific processes. For instance, Seine-Aval has a basin of stripping consisting in air injection. This air carries the most volatile compounds dissolved in water such as volatile organic pollution (trace of gasoline, solvent).

#### Primary treatment

The primary treatment removes the smallest particles in suspension by settling. One can add polymer in some specific basins (e.g. actiflo clarifier) in order to make coagulate the carbonaceous matter and to facilitate their removal. In some cases, metal salts like $FeCl_3$ are also added to precipitate compounds containing phosphorus. These precipitates are then removed with other particles.

#### Secondary treatment [1]

The secondary treatment removes organic compounds and nutrients that are dissolved in the water. During this treatment, bacteria consume biodegradable organic matter and nutrients for their growth.

The most common process is a treatment by activated sludge where bacteria are in suspension in the wastewater but they can also be fixed on a media. Concerning activated sludge process, the bacteria grow in the form of flocs in suspension. After a certain residence time, the wastewater and sludge mixture passes into a secondary decanter where the suspended matter is separated from the wastewater.

#### Tertiary treatment

The tertiary treatment aims to remove the remaining polluants, mainly phosphorus and nitrogen.Nitrogen removal, commonly done biologically, is done in two steps : nitrification and denitrification (more details in Section 1.2.2.4 & 1.2.2.3). Phosphorus can be biologicaly treated or with physico-chemical lamella settler (specific settler with add of metallic salts).

[1] In Seine-Aval, the pre-denitrification basin can be considered as a secondary treatment.

## 1.2 The Seine-Aval wastewater treatment plant

This section describes the specific case of the Seine-Aval wastewater treatment plant, its basins and its configuration. It then explains how each of these basins is modelised. The presented configuration of the Seine-Aval plan in based on [13].

### 1.2.1 Description

The plant is made of different bassins supporting a maximum flow (see Table 1.5):

- Physical-chemical settling tank with lamella.
- A biofiltration[2] and biological sludge treatment systems. The latter one is composed of three types of basins :
  - The pre-denitrification basins consist in (with the help of bacteria) transform the $NO_3^-$ into $NO_2^-$ and then in $N_2$ gas. The bacteria used consume carbon compounds in the same reaction. The utility of the pre-denitrification basin is to better treat the $NO_2^-$ and $NO_3^-$ via a recirculation ($u_r$) of the nitrification outflow (see scheme 1.1).
  - The nitrification basins transform the $NH_4^+$ into $NO_2^-$ and $NO_3^-$ that are then treated in the pre-denitrification and post-denitrification basins.
  - The post-denitrification basins placed downstream of the nitrification basins and implementing the same reaction as the pre-denitrification.

| Name | Type | Number | Volume/unit $[m^3]$ | Flow rate $[m^3/s]$ |
|---|---|---|---|---|
| Physico-chemical lamella settler | Densadeg | 25 | 2163 | 30 |
| Pre-denitrifying | Biostyr | 57+1 res. | 605 | 31.2 |
| Nitrifying | Biostyr | 84 | 605 | 45 |
| Post-denitrifying | Biofor | 11+1 res. | 441 | 11.2 |
| Clarifier | Actiflo | 9 | 3856 | 25 |

Table 1.5: Technical informations of Seine-Aval treatment plant

The plant has two configurations, below 30 $m^3/s$ for usual flows and above for very high flows. Depending on the configuration, the workflow of the plant is different.

[2]In the framework of this thesis, the biofiltration process will not be modelised since its flow is considered unsignificant compared to the average flow of the plant (2 $m^3/s$ vs 18.7 $m^3/s$ for the average flow of the plant).

**Flow rate $\leq$ 30 $[m^3/s]$**

When the station work in the usual flow mode, the flow of the waste water goes as follow (illustrated in Figure 1.1) :

1. The wastewater passes through a single Physical-chemical settling tank with lamella.
2. The wastewater goes then through biological sludge treatment systems composed of the pre-denitrification, the nitrification and the post-denitrification bassin.
3. The treated water then passes through a second Physical-chemical settling tank with lamella that acts as a clarifier.

There are a by-passes that allow to pass the pre-denitrification, post-denitrification and clarifier.

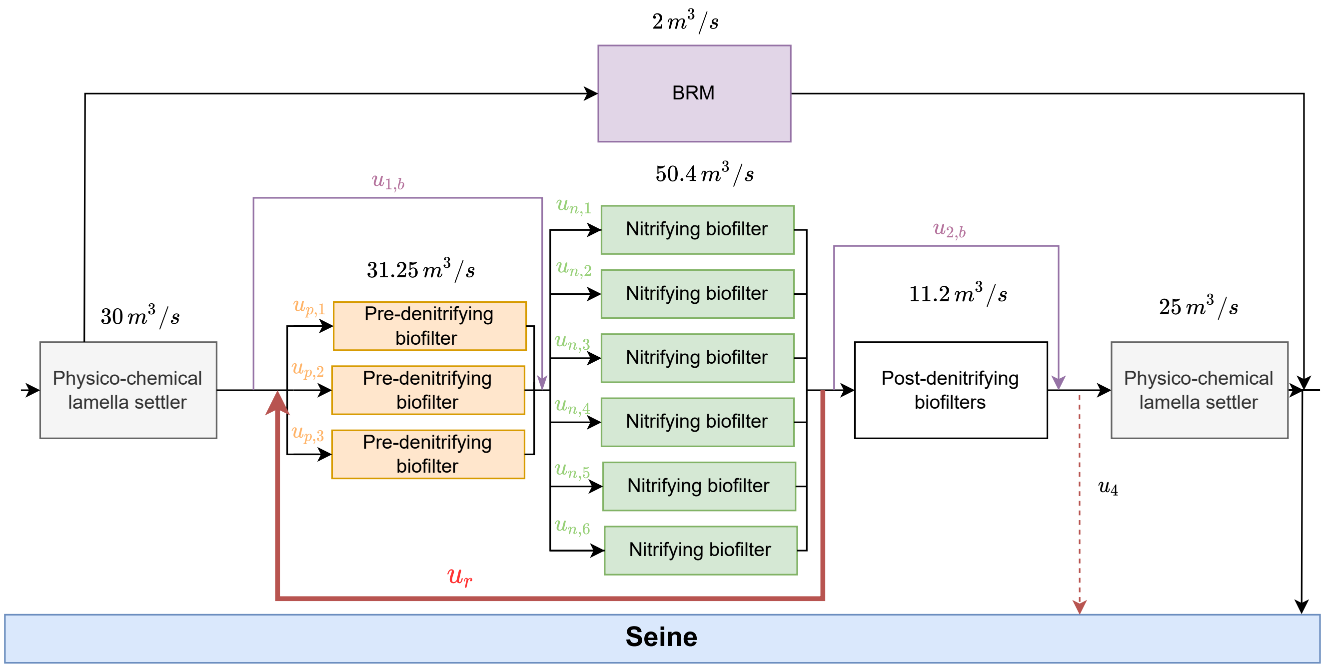


Figure 1.1: Scheme of the model used to represent Seine-Aval 2022 for flow rate $< 30m^3/s$

### Flow rate $\geq 30\ [m^3/s]$

When the flows are very important the configuration of the stations is slightly different. Here are the changes:

- Clarifiers are use for primary treatment
- Wastewater can be directly redirected at the exit of the plant (mixed before rejected) from the different sections to respect the flow limits

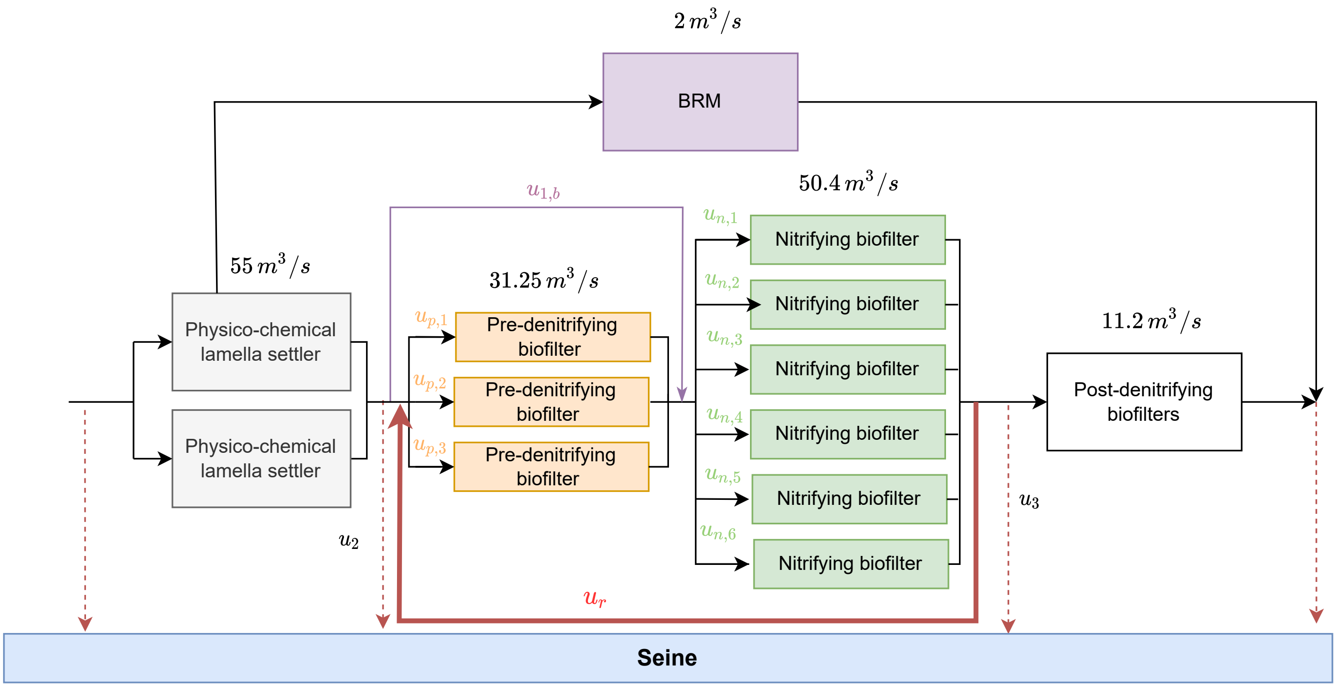


Figure 1.2: Scheme of the model used to represent Seine-Aval 2022 for flow rate $> 30m^3/s$

### Operating conditions

Figure 1.3 shows the average concentrations of the different pollutant measured daily from 2009 to 2014. It can be observed a clear decrease of $NO_3^-$ and an increase of $NO_2^-$ since 2013 corresponding to the implementation of the pre-denitrification stage. The performances concerning the nitrogen removal improve since this period as well. Before that, the standards for nitrogen discharge were not respected. Note also that the peak at day 800 of $NH_4^+$ is most likely due to the drought of summer 2011. The main information concerning the concentrations data are provided in Table 1.6.

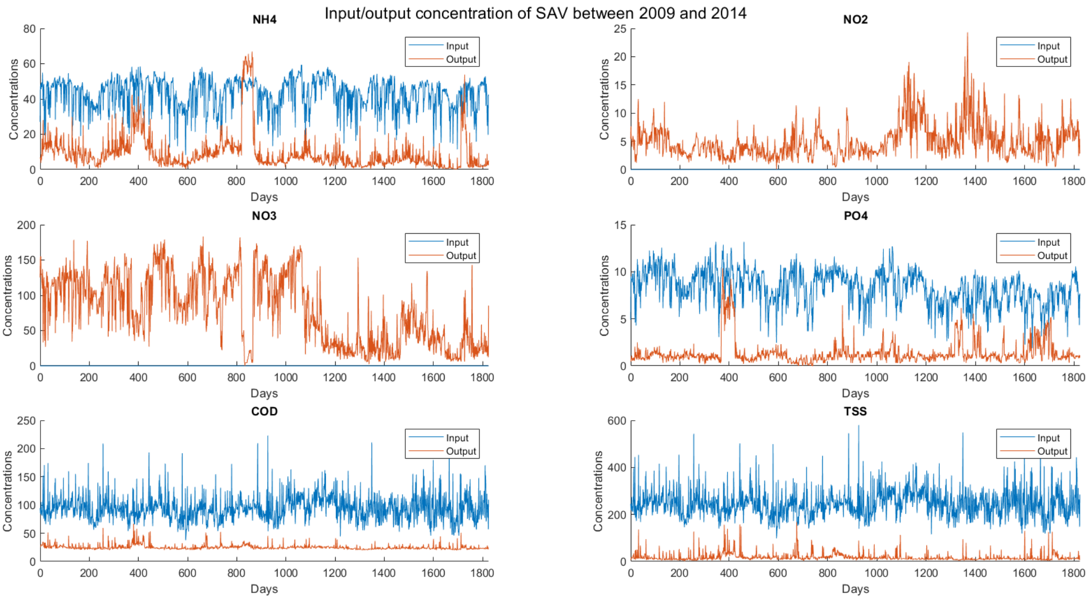


Figure 1.3: Concentrations upstream and downstream the Seine-Aval between 2009 and 2014 (one measurement per day)

| | | TSS | $BDO_5$ | $PO_4$ | $NH_4$ | $NO_2$ | $NO_3$ $[mg/L]$ | Q $[m^3/s]$ |
|---|---|---|---|---|---|---|---|---|
| Input | Mean | 244.5 | 180.8 | 8.3 | 42.8 | 0.0 | 0.0 | 18.7 |
| | Std | 56.7 | 34.0 | 1.8 | 8.6 | 0.0 | 0.0 | 4.4 |
| Output | Mean | 18.0 | 14.3 | 1.4 | 9.4 | 5.0 | 79.0 | 18.7 |
| | Std | 16.5 | 8.6 | 1.3 | 10.4 | 3.0 | 47.7 | 4.4 |

Table 1.6: Mean and standard deviation of input/outpout concentrations of Seine-Aval from 2009 to 2014

### 1.2.2 Model

This section begin with a general presentation of model use for bioreactor that are useful for the modelisation of the nitrification and denitrification unit. After that, the model for the physico-chemical settler is represented. Finally, the model for pre-denitrification, nitrification and post-denitrification are developed.

#### 1.2.2.1 General Dynamical Model of Bioreactor

A general state space model for biological process is presented on the basis of the book G.Bastin et al.[14] in Equation 1.1.

$$\frac{d\xi_i}{dt} = \sum_{j-i}(\pm)Y_{ij}\varphi_j - D\xi_i - Q_i + F_i \tag{1.1}$$

In this model $\xi_i$ are the $i$ components concentrations involved in the reaction scheme, $\varphi_j$ are the $j$ reaction rates and $Y_{ij}$ are the yield coefficient corresponding. $D$ is the dilution rate, $Q_i$ is the rate of the mass outflow of the component $\xi_i$ and $F_i$ is the feed rate in the reactor of the component $\xi_i$.

The reactions taking place in the biological process are several autocatalytic reactions involving two substrates (see Equation 1.2). The product of one reaction can be the substrate for other reaction.

The bacteria are both catalysts and products of the reaction. It is often considered that the concentration of bacteria $X$ is maintained in biological reactors[14]. One assume that the bacteria growth is equal to their disappearance by death.

$$S_1 + S_2 \xrightarrow[X]{\varphi} \mathrm{X} + \mathrm{P} \tag{1.2}$$

The reaction rate is express in Equation 1.3:

$$\varphi(S_1, S_2) \triangleq \mu(S_1, S_2)\mathrm{X} \tag{1.3}$$

$\mu$ is the bacteria growth rate and is modelised by the double Monod Equation 1.4.

$$\mu = \mu_{\max} \frac{S_1}{K_1 + S_1} \frac{S_2}{K_2 + S_2} \tag{1.4}$$

where $\mu_{\max}$ is the maximum growth rate, $K_1$ and $K_2$ are "Michaelis-Menten" constant (call also "Monod") and $S_1, S_2$ are substrate concentrations.

It is important to notice that the reaction scheme does not represent a stoichiometric relationship between the components. It simply represents a qualitative relation. This allows to include microbial growth,several not modeled or unknown process in a unique approach.

#### 1.2.2.2 Physico-chemical lamella settler

Physico-chemical lamella settler aims to remove solids from the treated water. Unlike the usual settling process, a series of metallic salts and polymers are added upstream of the settling tank. These components induce an increase in the flocculation of the particles by different mechanisms. This results in larger and denser particles in suspension that are easier to settle. As the physical-chemical settling tanks are more efficient, the size of the tanks can be reduced compared to the normal settling tanks.

Metal salts such as $FeCl_3$ have the added advantage of reacting with phosphate ions to produce different phosphorus precipitates, which are settled along with the other suspended solids. The efficiency of phosphate compounds varies between $65 - 95\%$ in the literature.

This mechanism was integrated in the ASM2 model of Henze et al (1999) [15]. The last works to date for the modeling of this process were carried out within the framework of the phase I of the MOCOPEE plan. These works allowed the development of the model Simdec [16].

A simpler model has also been developed by Ben Ayed et al.[5] based on the ASM models developed by the IWA. Here is a presentation of the latter model with the value of the variables presented in Table 2.8.

$$\frac{\mathrm{d[TSS]}}{\mathrm{d}t} = \frac{Q_{in}}{V_{set}}\left([\mathrm{TSS}_{in}] - [\mathrm{TSS}]\right) - k_0 \frac{[\mathrm{TSS}]\, u_1^r}{K_{FeCl_3} + u_1^r} \tag{1.5}$$

$$\frac{\mathrm{d[PO_4]}}{\mathrm{d}t} = \frac{Q_{in}}{V_{set}}\Big([\mathrm{PO}_{4,in}] - [PO_4]\Big) - k_1 \frac{[\mathrm{PO_4}]\, u_1^r}{K_{\mathrm{PO_4}} + [\mathrm{PO_4}]} \tag{1.6}$$

$$\frac{d[\mathrm{COD}]}{dt} = \frac{Q_{in}}{V_{set}}\left([\mathrm{COD}_{in}] - [\mathrm{COD}]\right) - k_2\, [\mathrm{COD}]\, [\mathrm{FeCl_3}] \tag{1.7}$$

| Parameter | Value | C.I. | Unit |
|---|---|---|---|
| $k_0$ | 82.85 | [68.1; 97.6] | $d^{-1}$ |
| $k_1$ | 2.04 | [1.88; 2.19] | $\mathrm{g_{PO_4}}/\mathrm{g}_{FeCl_3} d^{-1}$ |
| $k_2$ | 1.4 | [1.32; 1.47] | $m^3/\mathrm{g}_{FeCl_3} d^{-1}$ |
| $\mathrm{K_{PO_4}}$ | 0.0346 | [-4.89; 4.89] | $\mathrm{g_{PO_4}} m^{-3}$ |
| $\mathrm{K}_{FeCl_3}$ | $6.65\,10^{-7}$ | [0.021; 0.048] | $\mathrm{g}_{FeCl_3} m^{-3}$ |

Table 1.7: Calibrate parameter from reference article

#### 1.2.2.3 Pre-denitrification

Denitrification is the biological process of successively reducing $NO_3^-$ to $NO_2^-$ and then to $N_2$ (see Figure 1.4). These processes involve heterotrophic bacteria under anoxic conditions. Under these conditions these bacteria use assimilable carbon and oxygen from $NO_3^-$ and $NO_2^-$ for their growth. The global reaction is described by the Equation (1.8) [17].

$$6NO_3^- + 5CH_3OH \rightarrow 2\ N_2 + 5CO_2 + 7H_2O + 6OH^- \tag{1.8}$$

It has been observed that it is necessary to maintain a sufficient carbon supply to avoid an accumulation of $NO_2^-$. In a study carried out within the framework of the MOCOPEE project, it is advised to maintain a ratio Carbon/Nitrogen of 3 [18]. In order to maintain that ratio, methanol is introduced in the basins. In the developed model the methanol is not taken into account directly.

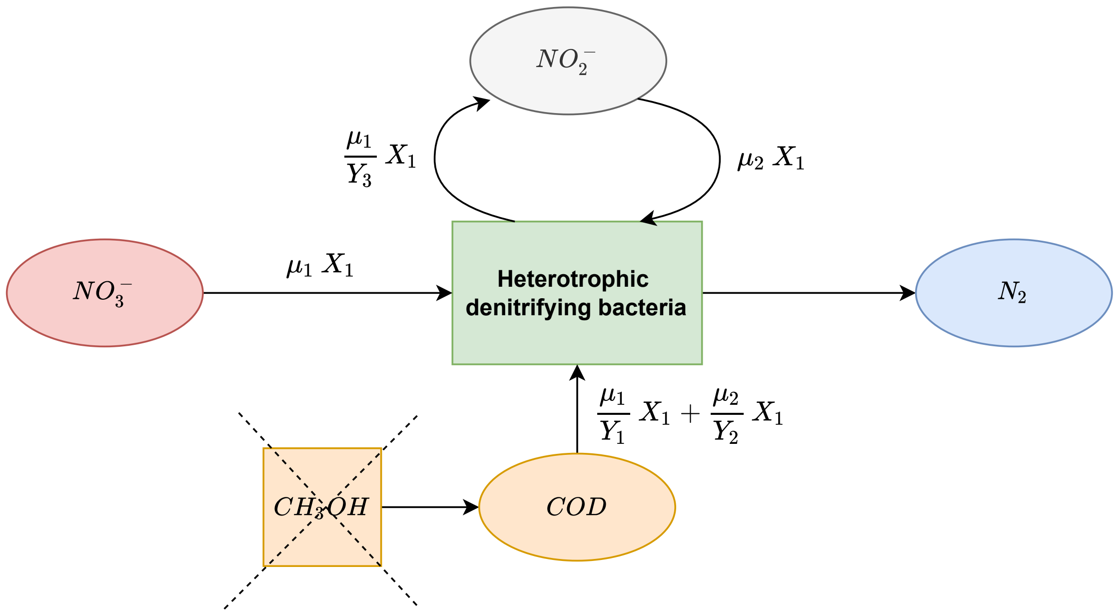


Figure 1.4: Scheme of the denitrification process

The following Equations 1.9 are derived from the standard model of biological processes [14]. It is assumed that there is no gas outflow or biomass variation (this parameter is considered as being of low order). Moreover, the impact of pH and temperature is not considered in this model.

$$\begin{aligned}
\frac{\mathrm{d[COD]}}{\mathrm{d}t} &= \frac{Q_{in}}{V}\left([\mathrm{COD}_{2,in}] - [\mathrm{COD}_2]\right) - \left(\frac{\mu_1}{Y_1} + \frac{\mu_2}{Y_2}\right) X_1 \\
\frac{\mathrm{d[NO_2]}}{\mathrm{d}t} &= \frac{Q_{in}}{V}\left([\mathrm{NO}_{2,in}] - [\mathrm{NO}_2]\right) + \left(\frac{\mu_1}{Y_3} - \mu_2\right) X_1 \\
\frac{\mathrm{d[NO_3]}}{\mathrm{d}t} &= \frac{Q_{in}}{V}\left([\mathrm{NO}_{3,in}] - [\mathrm{NO}_3]\right) - \mu_1 X_1
\end{aligned} \tag{1.9}$$

The reader should notice that the stochiometry of these equations give an order of magnitude but are not absolute. Indeed, since it is a simplified model, these equations do not represent all the involved reactions present.

The specific growth rates are modeled by double Monod equation, as follow:

$$\mu_1 = \mu_{1,\max}\frac{[\mathrm{COD}]}{K_{\mathrm{COD},1} + [\mathrm{COD}]}\frac{[\mathrm{NO_3}]}{K_{\mathrm{NO_3},1} + [\mathrm{NO_3}]} \qquad \mu_2 = \mu_{2,\max}\frac{[\mathrm{COD}]}{K_{\mathrm{COD},2} + [\mathrm{COD}]}\frac{[\mathrm{NO_2}]}{K_{\mathrm{NO_2},1} + [\mathrm{NO_2}]}$$

The calibration of this model has been done on Seine-Aval data between 08/2018 and 05/2019 by Ben Ayed et al. [5]. Table 2.8 shows the results of this calibration :

| Parameter | Value | C.I. | Typical value | Unit |
|---|---|---|---|---|
| $\mu_{1,max}$ | 0.072 | [0.044;0.099] | 3 | $g_{NO_3}/g_{X1}d^{-1}$ |
| $\mu_{2,max}$ | 50.8 | [-4.39;4.39] $10^5$ | 3 | $g_{NO_2}/g_{X1}d^{-1}$ |
| $Y_1$ | 0.077 | [0.04;0.69] | 0.2 | $g_{NO_2}/g_{O_2}$ |
| $Y_2$ | 0.14 | [0.11;0.18] | 0.3 | $g_{NO_3}/g_{O_2}$ |
| $Y_3$ | 40.57 | [22.2;235] | 1 | $g_{NO_3}/g_{NO_2}$ |
| $K_{NO_3,1}$ | 0.1 | [-0.14;0.34] | 0.5 | $g_{NO_3}m^{-3}$ |
| $K_{NO_2,1}$ | 0 | [-0.063;0.063] | 0.5 | $g_{NO_2}m^{-3}$ |
| $K_{COD,1}$ | 0 | [-21;21] | 0.1 | $g_{COD}m^{-3}$ |
| $K_{COD,2}$ | 8.24 $10^5$ | [-7.12;7.12] $10^9$ | 0.1 | $g_{COD}m^{-3}$ |

Table 1.8: Calibrate parameter from article Ben ayed et al [5]

#### 1.2.2.4 Nitrification

Nitrification consists in the transformation of $NH_4^+$ dissolved in $NO_3^-$ (see Figure 1.5). This transformation is done in two successive oxidation reactions involving nitrifying bacteria that draw their energy from it [19][20] :

1. **Nitritation** presented in Equation (1.10) involves ammonia-oxidizing bacteria (AOB).

$$NH_4{}^+ + 1.5O_2 \rightarrow NO_2{}^- + H_2O + 2H^+ \left(\Delta G^{0\prime} = -274.7 \text{ kJ mol}^{-1}\right) \quad (1.10)$$

2. **Nitration** presented in Equation (1.11)involves nitrite-oxidizing bacteria (NOB). These bacteria have a complex system of membranes containing enzymes, essential to the reactions that make up nitrification.

$$NO_2{}^- + 0.5O_2 \rightarrow NO_3{}^- \left(\Delta G^{0\prime} = -74.1 \text{ kJ mol}^{-1}\right) \quad (1.11)$$

Note that there are also bacteria (*nitrospira*) capable of doing both reactions. When these are in conditions where the concentration of substrate of the biofilm is low enough, the reaction become Equation (1.12):

$$NH_4{}^+ + 2O_2 \rightarrow NO_3{}^- + H_2O + 2H^+ \quad \left(\Delta G^{0\prime} = -348.9 \text{ kJ mol}^{-1}\right) \quad (1.12)$$

This direct reaction has only been updated recently and then is not implemented in the model. However, it still interesting to keep it in mind since it explains some behaviour of the model.

The reader should notice that the stochiometry of these equations give an order of magnitude but are not absolute. Indeed, since it is a simplified model, it does not represent all the involved reactions present. Specifically, they do not take into account the disappearance of reactional intermediates such as the $N_2O$ [13].

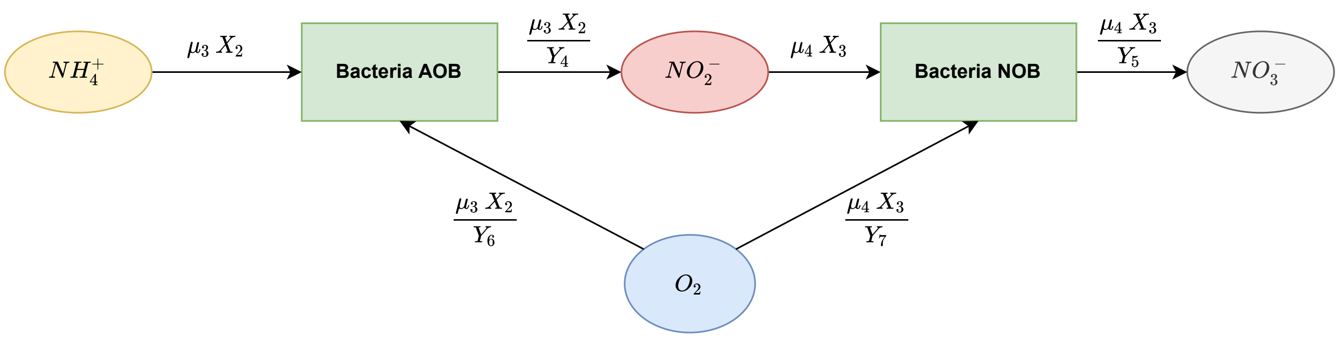


Figure 1.5: Scheme of the nitrification process

The following Equations 1.13 are derived from the standard model of biological processes [14]. It assumes no gas outflow or biomass variation (considered as being of low order). Moreover, the impact of pH and temperature are not considered.

$$\begin{aligned}
\frac{\mathrm{d}[\mathrm{NH_4}]}{\mathrm{d}t} &= \frac{Q_{in}}{V_{nitr}}\left([\mathrm{NH}_{4,in}] - [\mathrm{NH_4}]\right) - \mu_3 X_2 \\
\frac{\mathrm{d}[\mathrm{NO_2}]}{\mathrm{d}t} &= \frac{Q_{in}}{V_{nitr}}\left([\mathrm{NO}_{2,in}] - [\mathrm{NO_2}]\right) + \frac{\mu_3}{Y_4} X_2 - \mu_4 X_3 \\
\frac{\mathrm{d}[\mathrm{NO_3}]}{\mathrm{d}t} &= \frac{Q_{in}}{V_{nitr}}\left([\mathrm{NO}_{3,in}] - [\mathrm{NO_3}]\right) + \frac{\mu_4}{Y_5} X_3 \\
\frac{\mathrm{d}[\mathrm{O_2}]}{\mathrm{d}t} &= \frac{Q_{in}}{V_{nitr}}\left([O_{2,in}] - [\mathrm{O_2}]\right) - \frac{\mu_3}{Y_6} X_2 - \frac{\mu_4}{Y_7} X_3
\end{aligned} \tag{1.13}$$

The specific growth rates are modeled by double Monod equation, as follow:

$$\mu_3 = \mu_{3,\max}\frac{[\mathrm{NH_4}]}{K_{\mathrm{NH_4}} + [\mathrm{NH_4}]}\frac{[\mathrm{O_2}]}{K_{O_2,1} + [\mathrm{O_2}]} \qquad \mu_4 = \mu_{4,\max}\frac{[\mathrm{NO_2}]}{K_{\mathrm{NO_2},2} + [\mathrm{NO_2}]}\frac{[\mathrm{O_2}]}{K_{O_2,2} + [\mathrm{O_2}]}$$

The calibration of this model has been done on Seine-Aval data between 08/2018 and 05/2019 by Ben Ayed et al. [5]. Table 1.9 shows the results of this calibration:

| Parameter | Value | C.I. | Unit |
|---|---|---|---|
| $\mu_{3,max}$ | 1.67 | [1.5; 1.84] | $g_{NH_4}/g_{X3}d^{-1}$ |
| $\mu_{4,max}$ | 0.88 | [0.78; 0.96] | $g_{NO_2}/g_{X3}d^{-1}$ |
| $Y_4$ | 6.87 | [4.55;9.2] | $g_{NH_4}/g_{NO_2}$ |
| $Y_5$ | 0.14 | [0.09;0.20] | $g_{NO_2}/g_{NO_3}$ |
| $Y_6$ | 3.19 $10^5$ | [/;/] | $g_{NH_4}/g_{O_2}$ |
| $Y_7$ | 1.67 $10^5$ | [/;/] | $g_{NO_2}/g_{NO_2}$ |
| $K_{NH_4}$ | 0.01 | [-0.33;0.53] | $g_{NH_4}m^{-3}$ |
| $K_{NO_{2,2}}$ | 0.01 | [-1.42;3.59] $10^{-2}$ | $g_{NO_2}m^{-3}$ |
| $K_{O_{2,1}}$ | 1.5 $10^{-4}$ | [-2.25; 2.25] $10^3$ | $g_{O_2}m^{-3}$ |
| $K_{O_{2,2}}$ | 0 | [-0.7; 0.7] | $g_{0_2}m^{-3}$ |

Table 1.9: Calibrate parameter from article Ben ayed et al [5]

In view of the very low values of $K_{O_{2,1}}$ and $K_{O_{2,2}}$ the oxygen dependence of the model is neglected. This is due to the fact that the nitrification basins are properly aerated keeping the oxygen level at its saturation level.

#### 1.2.2.5 Post-denitrification

The reactions for the post-denitrification are almost the same as the pre-denitrification stage. They differ by the concentrations of the treated water. Also the model of filtration basins use Biofor for post-denitrification instead of Biostyr. The difference between these two filtration bassins resides in the media used to fix the bacteria. Equation 1.14 presents the reaction:

$$\begin{aligned}
\frac{\mathrm{d[COD]}}{\mathrm{d}t} &= \frac{Q_{in}}{V_{post}} \left([\mathrm{COD}_{in}] - [\mathrm{COD}]\right) - \frac{\mu_5}{Y_8} X_4 - \frac{\mu_6}{Y_9} X_4 \\
\frac{\mathrm{d[NO_2]}}{\mathrm{d}t} &= \frac{Q_{in}}{V_{post}} \left([\mathrm{NO}_{2,in}] - [\mathrm{NO_2}]\right) + \frac{\mu_5}{Y_{10}} X_4 - \mu_6 X_4 \\
\frac{\mathrm{d[NO_3]}}{\mathrm{d}t} &= \frac{Q_{in}}{V_{post}} \left([\mathrm{NO}_{3,in}] - [\mathrm{NO_3}]\right) - \mu_5 X_4
\end{aligned} \tag{1.14}$$

The specific growth rates are modeled by double Monod equation, as follow:

$$\mu_5 = \mu_{5,\max} \frac{[\mathrm{NO_3}]}{K_{\mathrm{NO_3},2} + [\mathrm{NO_3}]} \frac{[\mathrm{COD}]}{K_{\mathrm{COD},3} + [\mathrm{COD}]} \qquad \mu_6 = \mu_{6,\max} \frac{[\mathrm{NO_2}]}{K_{\mathrm{NO_2},3} + [\mathrm{NO_2}]} \frac{[\mathrm{COD}]}{K_{\mathrm{COD},4} + [\mathrm{COD}]}$$

The calibration of this model has been done on Seine-Aval data between 08/2018 and 05/2019 by Ben Ayed et al. [5]. Table 1.9 shows the results of this calibration:

| Parameter | Value | C.I | Typical value | Unit |
|---|---|---|---|---|
| $\mu_{5,max}$ | 576.97 | [184;970] | 3 | $g_{NO_3}/g_{X4}d^{-1}$ |
| $\mu_{6,max}$ | 0.31 | [-7.27;7.89] | 3 | $g_{NO_2}/g_{X4}d^{-1}$ |
| $Y_8$ | 0.25 | [0.17;0.45] | 0.2 | $g_{NO_2}/g_{COD}$ |
| $Y_9$ | 0.96 | [0.64;1.92] | 0.3 | $g_{NO_3}/g_{COD}$ |
| $Y_{10}$ | 27.57 | [20.2;43.6] | 1.35 | $g_{NO_3}/g_{NO_2}$ |
| $K_{NO_{3,2}}$ | 0.1 | [-0.008;0.21] | 0.5 | $g_{NO_3}m^{-3}$ |
| $K_{NO_{2,3}}$ | 0 | [-5.3.;5.3] | 0.5 | $g_{NO_2}m^{-3}$ |
| $K_{COD,3}$ | 70.29 | [-7.88;148] | 0.1 | $g_{COD}m^{-3}$ |
| $K_{COD,4}$ | 0.001 | [-806;806] | 0.1 | $g_{COD}m^{-3}$ |

Table 1.10: Calibrate parameter from reference article Ben ayed et al [5]

## 1.3 Optimisation method

Here, one presents the theoretical framework related to the optimization of the system. This section refers to the book Numerical Optimization of Nocedal et al.[21].

First of all, a mathematical definition of an optimization problem is given. Then, it presents different algorithms that solve non-linear optimization problems with constraints. Finally, the objective function is explained.

### 1.3.1 Mathematical formulation

Optimization is defined as the minimization or maximization of a function that can be under constraints. The following notations are used in this section:

- **x** is the **variables**, in this work it is the control variables.
- $f$ is the **objective function**, a function of **x** to be optimized. Section 1.3.3 details it.
- $c_i$ are **constraint function**, these impose relation that **x** must statisfy.

Then, the optimization problem is described in Equation 1.15:

$$\min_{x \in \mathrm{R}^n} f(x) \quad \text{subject to} \quad \begin{array}{ll} c_i(x) = 0, & i \in \mathcal{N}, \\ c_j(x) \geq 0, & j \in \mathcal{M}. \end{array} \tag{1.15}$$

where $\mathcal{N}$ and $\mathcal{M}$ are set the indices for equalities and inequalities constraints.

The optimality conditions are defined as follow:

- **Necessary conditions**: Local unconstrained minimizers have $\nabla f(x^*) = 0$ and $\nabla^2 f(x^*)$ positive semidefinite.
- **Sufficient conditions**: Any point $x^*$ at which $\nabla f(x^*) = 0$ and $\nabla^2 f(x^*)$ is positive definite, is a strong local minimizer of $f$.

If all the constraints and the objective function are linear functions of **x** the problem is a linear programming problem. If not, the problem is called "Nonlinear Programming Problems".

Many nonlinear optimization reach only local solution, i.e. a value of the objective function that is smaller than for all the other nearby points. Local solution are not always global solution, i.e. a value of the objective function that is smaller than all the other points of variable space. A local optimum can be considered as global optimum only for **convex programming** problems.

Convex programming defines a constrained optimization problem with the following characteristics:

- The objective function is convex.
- The equality constraint functions $c_{i \in \mathcal{N}}$ are linear.
- The inequality constraint functions $c_{j \in \mathcal{M}}$ are concave.

Optimization algorithms are iterative. They start with one or multiple guess for the variables $\mathbf{x}$ and iterate through a series of better estimates until they reach a solution.

One algorithm differs from another due to the strategy used to move from one iteration to the next one. The values of the objective function $f$, the constraint functions $c_i$, and possibly the first and second derivatives of these functions are used in most strategies.

Algorithms are often categorized according to whether they use the objective function derivative and whether they start with one or more points.

To sum up, optimisation problem with constraint can be written as follow:

$$\Omega = \{x \mid c_i(x) = 0, \quad i \in \mathcal{N}; \quad c_j(x) \geq 0, \quad i \in \mathcal{M}\} \tag{1.16}$$

$$\min_{x \in \Omega} f(x) \tag{1.17}$$

### 1.3.2 Optimisation for constraint problem

After a review of the litterature, **Sequential Quadratic Programming (SQP)** and **Genetic Algorithm (GA)** were selected as the optimization algorithm. Note that Boomgaard et al. already used GA for the optimization of wastewater treatment systems [22] and Benthack et al. used SQP to optimize the operation strategy of a bed-fixed bioreactor [23]. These 2 algorithms are introduced below.

#### Genetic algorithm

The following description of Genetic Algorithm is based on the book [24] and the Matlab Documentation [25]. The Genetic Algorithm is inspired by the principle of natural evolution. The steps followed by the program are described below:

1. Create random initial population of point.
2. Evaluate each point with the objective function.
3. Select members as parents based on the value of the objective function.
4. Keep the best member for the next generation.
5. Produce new point ("Children") by making random change to a single parent ("Mutation") or by combining a pairs of parents ("Crossover").
6. Replace the current population with the children.
7. Iterate this procedure until the stopping criteria is met.

The algortihm used in this work is the implementation of genetic algorithm available in Matlab Software [26]. The number of direct selected member for the next generation and the fraction of cross over are parameter of the algorithm.

#### Sequential quadratic programming

Sequential Quadratic Programming approach can be used for large constrained problem. This problems need derivative or approximate derivative of the objective function. This algorithm work by solving quadratic sub-problems and iterate. More details can be found in this book [21].

The implementation of the algorithm is provided by Matlab software [26].

### 1.3.3 Objective function for WWTP

The development of global indices to describe wastewater treatment quality is an important topic in the optimization of treatment systems.

A study by Vanrolleghem et al.[27] focuses on the development and use of such indices. This article develop two indices that are used in Flanders and Denmark as legislation. From this work, an index that take into account the operational costs of the stations was designed in 2002 in the article of Vanrolleghem et al. [28]. This index has then been slightly modified and used in the work of Guerrero et al.[29].

In general, all these indices involve weighted sums of effluent concentrations and operational costs. The definitions of the weights are still under debate. A recent work by Nezhad et al.[30] focuses on redefining the weights.

For this work it was decided to focus on water quality. The objective function is the effluent quality index (EQI) defined in the Equation 1.18. The reason such a simple weighted sum is to try to make this function smooth reasonably predictable. This allows algorithms to search in the right direction.

$$EQI = \frac{1}{10^6 t_{obs}} \int \sum (\beta_i * \text{Pollutant}_i) * Q_{\text{effluent}} dt \tag{1.18}$$

Jialu [13] redefined the weights as a fonction of the polluant. This was done on the basis of the Nopens et al. paper [31]. The weights assigned to the nitrogenous pollutants have been modified to have an equal impact with respect to the nitrogen weights of the pollutants. Their values are provided in Table 1.11.

| Pollutants | Weight | New Weight |
|---|---|---|
| COD | 6 | 35 |
| TSS | 10 | 10 |
| $NH_4^+$ | 30 | 35 |
| $NO_3^-$ | 10 | 10 |
| $NO_2^-$ | 20 | 14 |
| $PO_4$ | 20 | 20 |

Table 1.11: Pollutants and weight factor use for EQI

## Conclusion

This section started by giving an introduction to wastewater treatment. Then it details a description of the Seine-Aval wastewater treatment plant. From this, a simplified model of the Seine-Aval is described based on Ben ayed et al.[5]) This uses the activated sludge models (ASM). After, a rigorous mathematical formulation of an optimization problem was given. Finally, one presented the optimization algorithms used in this work.

# Chapter 2

# Model implemantation

## Introduction

Firstly, this section presents the structure of the code implementing the model. Then, the different models are calibrated to fit the bacteria concentration. After, the quality of the model is tested. If necessary some parameters are re-calibrated. In this section re-calibration or new calibration is used to say that the parameters used by Ayed et al.[5] are modified according to the available data.

## 2.1 Code description

The model is implemented with Matlab [26]. Its two big advantages is to propose a graphical interface to visualize the signals (via Simulink) and it is very efficient for the resolution of differential equation. The code is available on Github.

The program used is composed of three types of blocks :

- **The integrator block :** It integrates the differential equations provided to it. This block takes as input a Timeseries "Flow" containing the concentrations and the input mass flow of the modeled section. It also takes the initial concentrations of the basin. The output of this block contains a new Timeseries of type "Flow" with the concentrations of outputs.

- **The valve block :** It splits the flow into N parts. It takes as input a Timeseries Flow and a vector containing the value of the flow of the N parts. It gives as output N new Timeseries with the same concentrations as the input flow but with the desired flow.

- **The Mix Block :** It takes N Timeseries as input and outputs a Timeseries containing the flow corresponding to the mix of the N input flows.

As an example, the Simulink diagram used to simulate the wastewater treatment plant when the flow rate is less than 30 $[m^3/s]$ is shown on Figure 2.1.

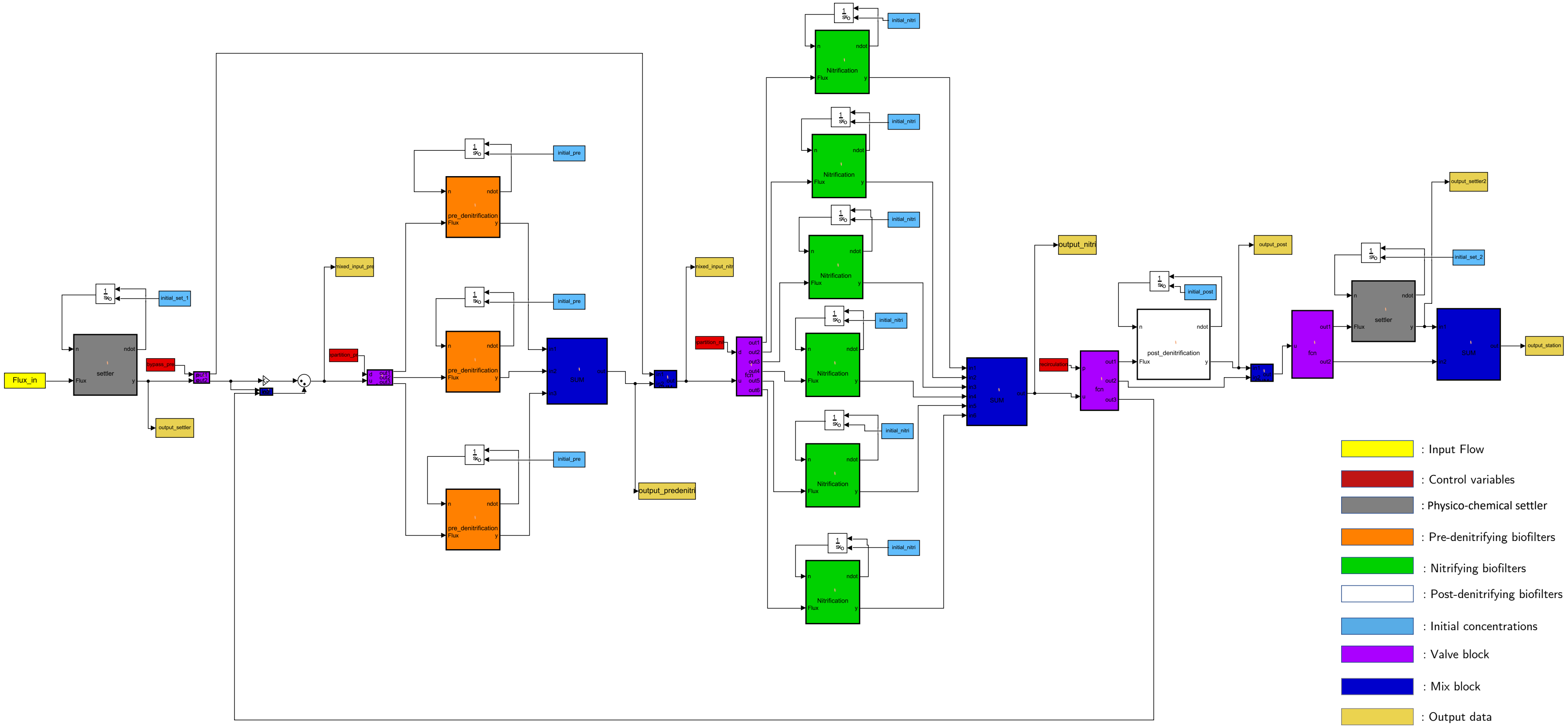


Figure 2.1: Simulink model of Seine-Aval 2022 for $Q < 30\,m^3/s$

## 2.2 Physico-chemical lamella settler

In this part, the implementation of the model for the physico-chemical lamella settler is verified. Following this results, a verification a re-calibration is proposed.

### 2.2.1 Data

The verification of the block and its implementation were based on the information available in the thesis of Jialu [13]. In this thesis, physico lamella settler is calibrated on data from the Seine Centre wastewater treatment plant (between 2000 and 2008). In this wastewater treatment plant there is 15 Densadeg physico lamella settler of 2163 $m^3$.

The main information's on this data are given in Table 2.1. It is the same data used for the calibration of SimDec model [16] which is the most accurate model to date for physico-chemical lamella settler.

| | | TSS | $PO_4$ | COD | $FeCl_3$ $[mg/L]$ | Q $[m3/s]$ |
|---|---|---|---|---|---|---|
| Input | Mean | 206.5 | 2.5 | 347.8 | 32.6 | 78736 |
| | Std | 59.2 | 0.6 | 88 | 6 | 7575 |
| Output | Mean | 25.7 | 0.34 | 114.9 | / | 78736 |

Table 2.1: Main operating conditions of the physico-chemical lamellar decanters of the Seine Centre wastewater treatment plant from 2000 to 2008

### 2.2.2 Results

Concerning the simulation, the initial concentrations is put to the data average output concentrations. And the input signal is set to the input data given in Table 2.1. The equilibrium concentrations are available in the Table 2.2.

| | TSS | $PO_4$ | COD | Units |
|---|---|---|---|---|
| Model output | 61.3 | 0.73 | 176.42 | $[mg/L]$ |
| Mean Data output | 25.7 | 0.34 | 114.9 | $[mg/L]$ |

Table 2.2: Mean output concentration of the physico-chemical lamellar decanters of the Seine Centre wastewater treatment plant from 2000 to 2008

The equilibrium concentrations reached by the model are different from those expected. Without more information about the parameters than the one given in [5] it then difficult to give a reliable explanation about the origin this error.
It is therefore decided to re-calibrate the model.

### 2.2.3 New calibration

The calibration consists in tuning the parameters such that for the data input (see Table 2.1) the model reach the average output concentration (see Table 2.2). It is possible to find new values of the parameters analytically using Equations 2.1 :

$$\begin{aligned} k_0 &= \frac{Q_{\text{in}}}{V_{\text{set}}} \frac{([\text{TSS}_{\text{in}}] - [\text{TSS}_{\text{out}}])}{\text{TSS}_{\text{out}}} = 256.75 \\ k_1 &= \frac{Q_{\text{in}}}{V_{\text{set}}} \left([\text{PO}_{4,\text{in}}] - [\text{PO}_{4,\text{out}}]\right) \frac{K_{\text{PO}_4} + [\text{PO}_{4,\text{out}}]}{[\text{PO}_{4,\text{out}}]\, u_1^r} = 2.66 \\ k_2 &= \frac{Q_{\text{in}}}{V_{\text{set}}} \frac{([\text{COD}_{\text{in}}] - [\text{COD}_{\text{out}}])}{[\text{COD}_{\text{out}}]\,[\text{FeCl}_3]} = 2.27 \end{aligned} \tag{2.1}$$

This new calibration is not optimal as it is based on too little information. It is not sure that the model represents the situation correctly. However, it has the advantage of returning consistent values that are useful for the next block of the wastewater treatment plant.

## 2.3 Nitrification and post-denitrification

This section starts by presenting the available data for the nitrification and post-denitrification stages. Then, the bacterial concentrations of these two units are calibrated on this data set.

Given the bad results obtained, some of the constants of the model are calibrated on the data set. Finally, the results obtained with the new parameters are analyzed.

### 2.3.1 Data

The only accurate data available are the daily averages of the inlet and outlet of Seine-Aval between 2009 and 2014 (see Table 2.3).

| | | COD | $NH_4$ | $NO_2$ | $NO_3$ $[mg/L]$ | Q $[m3/s]$ |
|---|---|---|---|---|---|---|
| Input | Mean | 93 | 44.94 | 0 | 0 | 19.48 |
| | Std | 8.96 | 7.49 | 0.0 | 0.0 | 4.21 |
| Output | Mean | 60.84 | 13.24 | 5.7 | 107.78 | 18.7 |
| | Std | 7.62 | 4.49 | 2.1 | 26.57 | 4.21 |

Table 2.3: Mean and standard deviation of input/outpout concentrations of the Seine-Aval from 2009 to 2014

In 2011, some work were made to modernise the station. It aims to do a complete overhaul of the pre-treatment plant. The data after 2011 are therefore difficult to treat because the state of the station is changing (closure of section for works, start-up ...).

Therefore, it is decided to use the 2009 data for the verification and calibration of the nitrification and post-denitrification units.

The nitrification and post-denitrification sections were reproduced in Simulink according to the 2009 configuration (see Figure 2.2 and Table 2.4). The disposition of the measurements are also shown in the Figure 2.2.

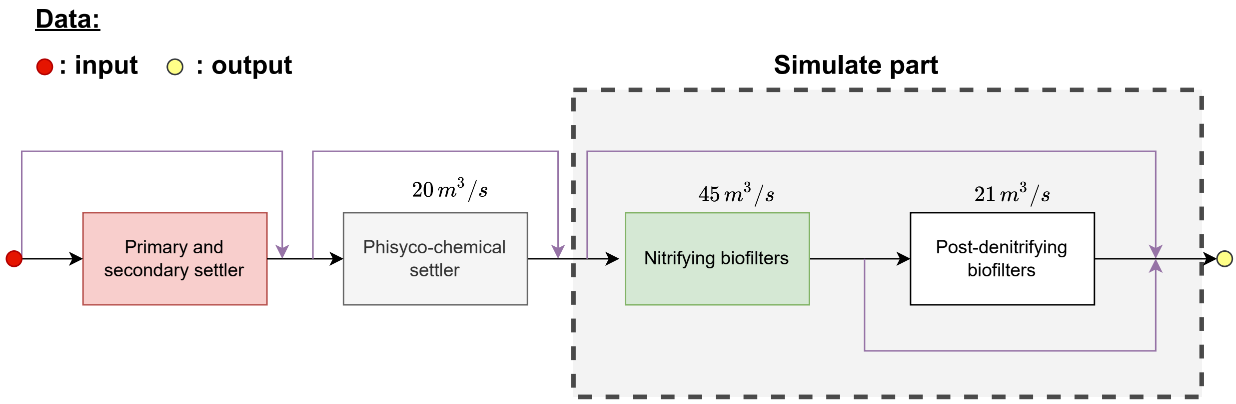


Figure 2.2: Scheme of the configuration of the Seine-Aval plant in 2012

| Name | Type | Number of units | Volume/unit $[m^3]$ | Max. Flow rate $[m^3/s]$ |
|---|---|---|---|---|
| Nitrifying biofilters | Biofor | 84 | 605 | 45 |
| Post-denitrifrifying biofilters | Biofor | 12 | 441 | 21 |
| | Biostyr | 18 | 605 | |

Table 2.4: Equipment of the simulator part of the Seine-Aval wastewater treatment plant in 2012 [32]

For $NH_4^+$, $NO_2$ and $NO_3$ the concentration values at the entrance of the simulated section are the same as those at the entrance of the station. For COD, this is not the case. The input signal of COD concentration was therefore normalized and then multiplied by the average value of the input in 2009 of the nitrification stage given in [13].

Ideally, input and output data from each section would have been required as for the calibration and validation of the model developed by Jalhu.

### 2.3.2 Calibration

To allow the calibration of the bacterial concentrations $X_2$,$X_3$ and $X_4$, a model of the 2009 wastewater treatment plant was reconstructed according to the description made previously (see Figure 2.2).

The calibration is based on the minimization of an objective function with the alogrithm `fminsearch()` of Matlab. The objective function used is a normalized mean squared error defined in Equation 2.2:

$$\text{NMSE} = \sum_{d=1}^{N} \sum_{i=1}^{T} \frac{(C_{\text{data},d,i} - C_{\text{model},d,i})^2}{\overline{C_{\text{data},d}}^2 \, T \, N} \tag{2.2}$$

The model is used as a black box to calculate the NMSE. The minimization problem can be write in the following form.

$$\text{NMSE} = f(X_2, X_3, X_4) \tag{2.3}$$

$$\min(\text{NMSE}) \tag{2.4}$$

The result for the bacteria concentration are given in Equation 2.5:

$$X_1 = 416\,[g/m^3] \qquad X_2 = 2747\,[g/m^3] \qquad X_3 = 3000\,[g/m^3] \tag{2.5}$$

From Bernier et al.[17] a usual bacteria concentration is around 1250 $[g/m^3]$. The result obtained are far from that. Nevertheless these values remain in a acceptable range.

It is not possible to guarantee that the value find are a global minimum. Other minimization algorithms have been tested and give comparable results with slightly different values.

### 2.3.3 Results

In the following, the results are presented for the output of the nitrification, as well as for the post-denitrification.

### Nitrification

The concentrations output predicted by the model for the nitrification section are shown in Figure 2.3. Their averages and their differences from the average data values are presented in Table 2.5 and in Table 2.6 respectively.

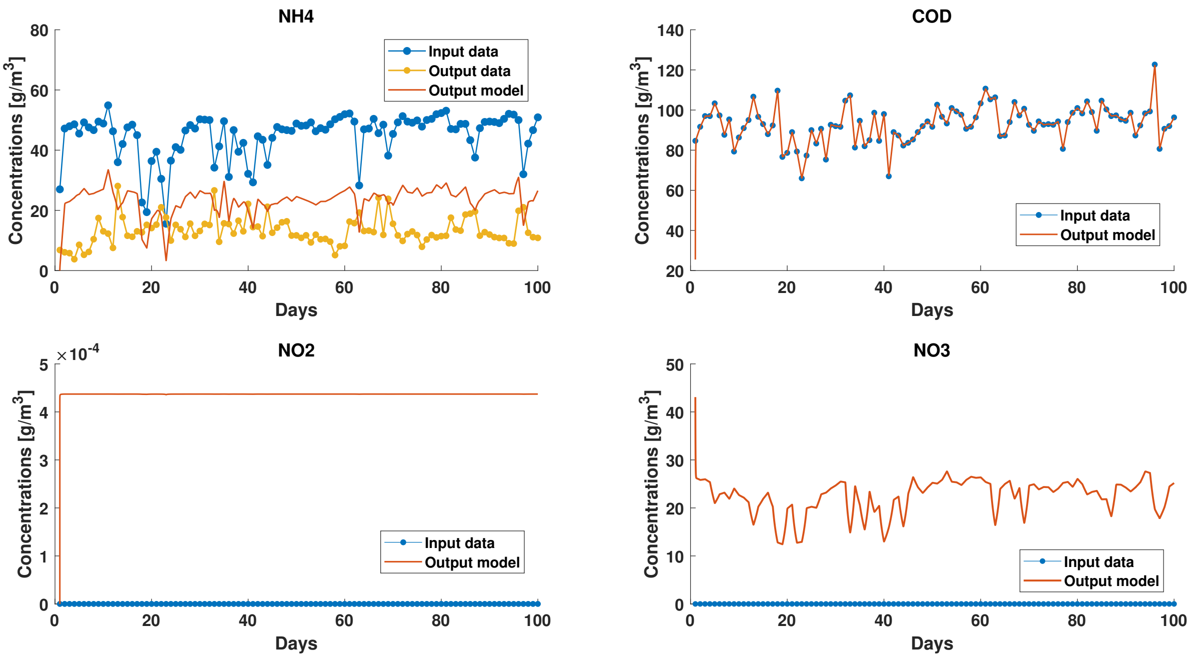


Figure 2.3: Simulated input/output concentration for the nitrification in 2009

| | $NH_4$ | $NO_2$ | $NO_3$ $[mg/L]$ |
|---|---|---|---|
| Mean output | 7.13 | 2.56 | 142 |

Table 2.5: Mean output concentrations of nitrification stage for 2009 [13]

| | $NH_4$ | $NO_2$ | $NO_3$ $[mg/L]$ |
|---|---|---|---|
| Mean | 21.35 | 0 | 23.35 |
| Error on mean | 14.22 | -2.56 | -118.6 |

Table 2.6: Mean and error of the output concentrations at the nitrification

The results are not good (see Table 2.6). None of the output values of the model are close to the expected values, especially for the concentration of $NO_2$ which is zero, which never happens in reality.

### Post-denitrification

Figure 2.4 shows the predicted output concentrations for the post-denitrification.

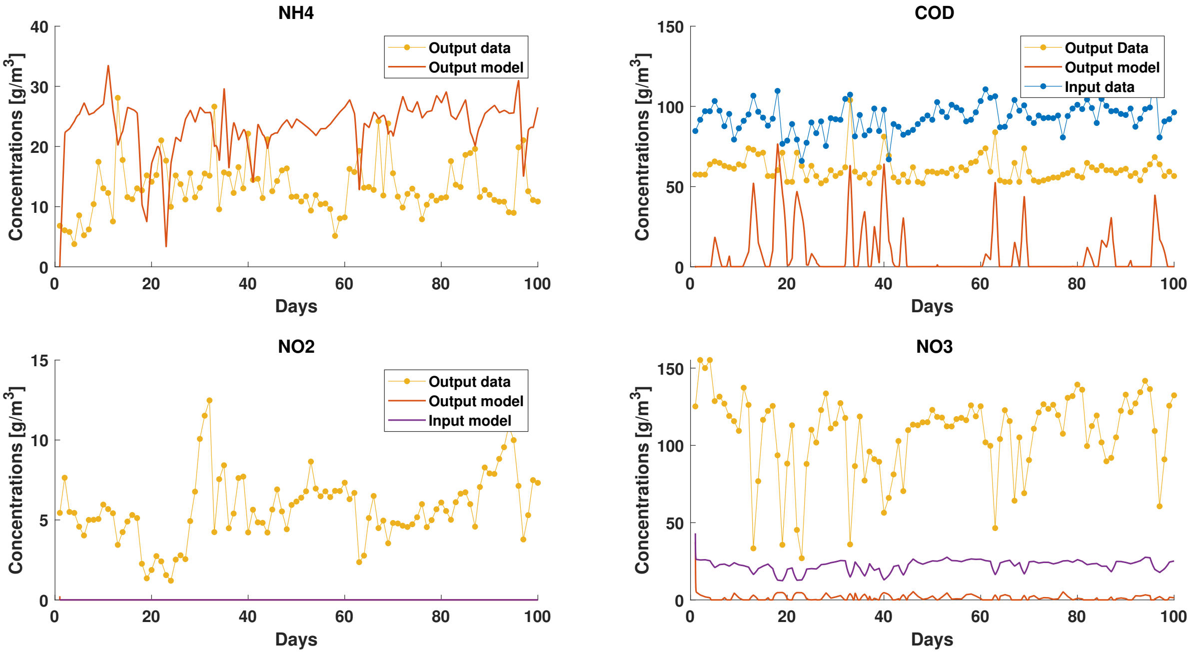


Figure 2.4: Input and output concentration of the simulation for Seine-Aval WWTP in 2009

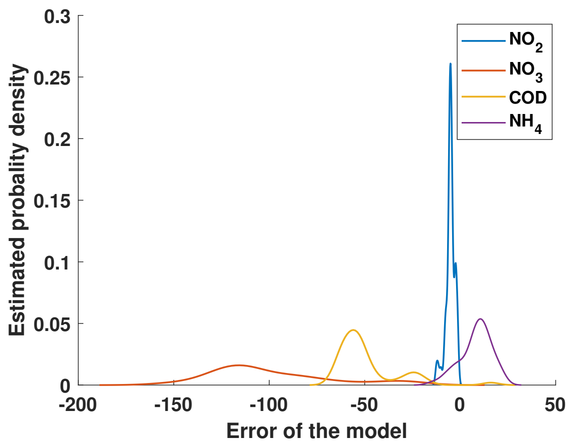


Figure 2.5: Estimate distribution of the model error

The main information about the model error are presented in the Table 2.7.

| | COD | $NH_4$ | $NO_2$ | $NO_3$ $[mg/L]$ |
|---|---|---|---|---|
| ME | -52 | 10 | -5.7 | -105.5 |
| ME c.i. | [-49.8 -54.2] | [8.8 11.2] | [-6.0 -5.3] | [-110 -101] |
| ME std | 13.2 | 7.2 | 2.1 | 27.04 |
| MAE | 52.3 | 11.2 | 5.7 | 105.5 |
| MSE | 53.6 | 12.3 | 6.0 | 108.8 |
| $R^2$ | -6.75 | -7.2 | -16 | -47.7 |

Table 2.7: Statistical score results for the nitrification and post-denitrification stage simulation in 2009

As it can be seen in the Figure 2.4 and on the Figure 2.5 the model is completely out of order.The main reason for this problem is that the calibration is based on data from 2018 to 2019. According to Jialu's thesis [13], there were problems with the representativeness of the measurements during these years. This explains some unexpected values of parameters for the post-denitrification. More details will be given in the next section.

### 2.3.4 New calibration

In the view of the unsatisfactory result obtained in the previous section it is decided to re-calibrate the parameters of the nitrification and denitrification models. Two attempts were conducted.

#### First attempt

As only the inlet and outlet of the station are known, the post-denitrification and nitrification stages will be calibrated together. The problem with this approach is the large number of parameters to be calibrated, i.e. 16 (see Table 1.9 and Table 1.10). Normally, a way to reduce the number of parameters calibrated simultaneously is to calibrate first the yield coefficients by using the principle of reaction invariant. However, without the output data of the nitrification stage this calibration is impossible.

Two calibrations on the set of parameters are then tried using the Matlab function `fminsearch()` and `lsqnonlin()`. `fminsearch` uses simplex search method while `lsqnonlin` use Levenberg-Marquardt method based on Gauss-Newton and Gradient-Descent Algorithm.

The results are not conclusive due to the dimension of the parameters space to explore. Also, one assume that the method fall into a local minimum.

#### Second attempt

Given the bad results of the first attempt, a second attempt is conducted. The strategy is to identify the problematic parameters thanks to the knowledge of the model. It is also decided to modify as little as possible the parameters of the nitrification model.

The problems of the nitrification simulation are shown Table 2.6. There are a too low consumption of $NH_4$ and a too low production of $NO_3$ and $NO_2$. As one can see on Figure 2.3, even if the consumption of $NH_4$ is lower than the one expected, it is not unsignificant compared to the one of $NO_2$. The factor linking the consumption of $NH_4$ and $NO_2$ is $Y4$ (see Figure 1.5).

The parameters of the nitrification model kept for the calibration are therefore $Y_4, X2$ and $X3$. For the post-denitrification all the parameters are kept for the calibration except the redundant one that is $X_4$ that multiplies $\mu_{5,\text{max}}$ and $\mu_{6,\text{max}}$. Altogether, this gives the following minimization problem:

$$\text{NMSE} = \sum_{d=1}^{N} \sum_{i=1}^{T} \frac{(C_{\text{data},d,i} - C_{\text{model},d,i})^2}{\overline{C_{\text{data},d}}^2\, T\, N} \tag{2.6}$$

$$\text{NMSE} = f(X_2, X_3, Y_8, Y_9, Y_{10}, \mu_{\text{max},5}, \mu_{\text{max},6}, \text{K}_{\text{NO}_{3,2}}, \text{K}_{\text{NO}_{2,3}}, \text{K}_{\text{COD},3}, \text{K}_{\text{COD},4})$$

$$\min(\text{NMSE})$$

To solve this problem the algorithms `fmicon()` and `ga()` have been used again. The best combination of parameters found is given in the Table 2.8.

| Parameter | Value | New value | Typical value | Unit |
|---|---|---|---|---|
| $X_2$ | / | 640 | 1250 | $\text{g}_{\text{bacteria}} m^{-3}$ |
| $X_3$ | / | 634 | 1250 | $\text{g}_{\text{bacteria}} m^{-3}$ |
| $\mu_{5,\text{max}}$ | 576.97 | 3.95 | 3 | $\text{g}_{\text{NO}_3}/\text{g}_{X4} d^{-1}$ |
| $\mu_{6,\text{max}}$ | 0.31 | 1.99 | 3 | $\text{g}_{\text{NO}_2}/\text{g}_{X4} d^{-1}$ |
| $Y_4$ | 6.87 | 1.87 | 0.4 | $\text{g}_{\text{NH}_4}/\text{g}_{\text{NO}_2}$ |
| $Y_8$ | 0.25 | 0.675 | 0.2 | $\text{g}_{\text{NO}_2}/\text{g}_{\text{COD}}$ |
| $Y_9$ | 0.96 | 0.9 | 0.3 | $\text{g}_{\text{NO}_3}/\text{g}_{\text{COD}}$ |
| $Y_{10}$ | 27.57 | 0.96 | 1.35 | $\text{g}_{\text{NO}_3}/\text{g}_{\text{NO}_2}$ |
| $\text{K}_{\text{NO}_{3,2}}$ | 0.1 | 0.4 | 0.5 | $\text{g}_{\text{NO}_3} m^{-3}$ |
| $\text{K}_{\text{NO}_{2,3}}$ | 0 | 1.05 | 0.5 | $\text{g}_{\text{NO}_2} m^{-3}$ |
| $\text{K}_{\text{COD},3}$ | 70.29 | 71.5 | / | $\text{g}_{\text{COD}} m^{-3}$ |
| $\text{K}_{\text{COD},4}$ | 0.001 | 11.6 | / | $\text{g}_{\text{COD}} m^{-3}$ |

Table 2.8: Calibrated parameters

$X_4$ is set to the value allowing to have the values of $\mu_{\text{max},5}$ and $\mu_{\text{max},6}$ closest to the typical values. The result is:

$$X_4 :\ 761.3\,[g\,m^{-3}] \tag{2.7}$$

Even if this optimization does not allow to find a global optimum but it has the advantage to find coherent values. Figure 2.6 shows the results of the simulation of the first 100 days of the year 2009 (calibration period).

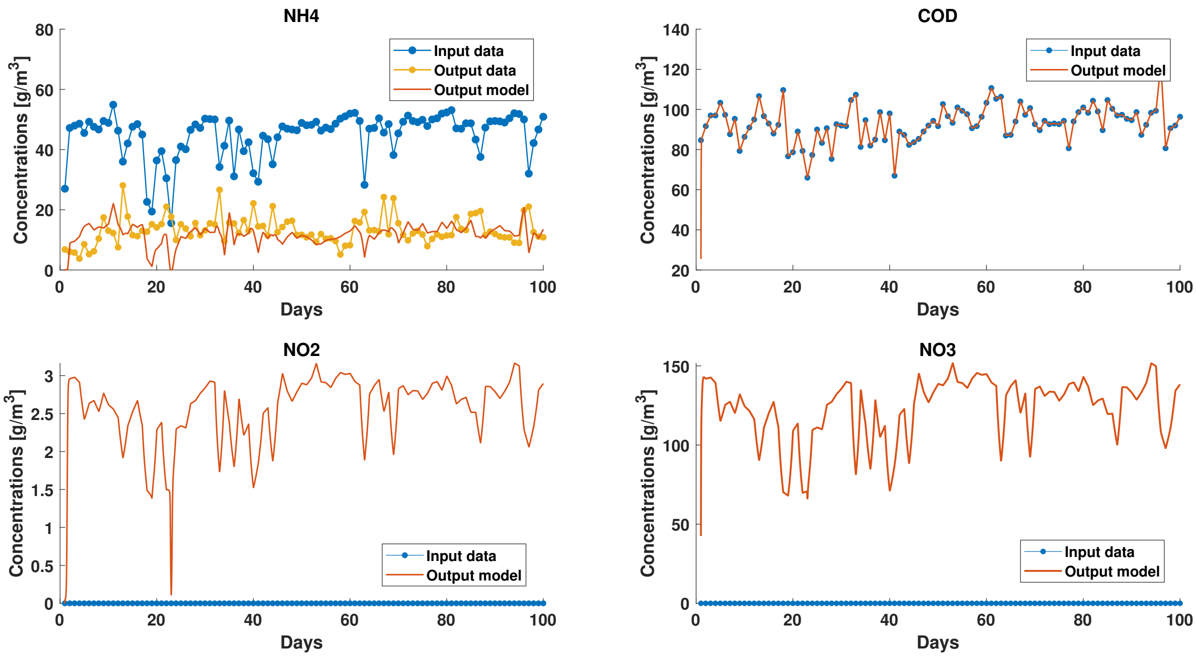


Figure 2.6: Input and output concentration of the simulation with new parameters for the nitrification stage in 2009

The main results and the plot of the concentrations for the validation period are given in Appendix A. The results for validation period are comparable to the one of the calibration period.

The average and the error on the average of the concentrations at the exit of nitrification stage are given in the Table 2.9.

| | $NH_4$ | $NO_2$ | $NO_3$ $[mg/L]$ |
|---|---|---|---|
| Mean | 10.32 | 2.05 | 114.53 |
| Error on mean | 3.19 | 0.41 | -27.57 |

Table 2.9: Mean and error on mean of the output concentrations give by the model for data of the Seine-Aval 2009

With the new calibration the $NO_2$ and $NO_3$ concentrations reach much more credible values. Indeed, the decrease of the $Y_4$ factor results in an increase of the $NO_2$ production for the same $NH_4$ consumption. With a much higher concentration of $NO_2$ the production of $NO_3$ is no longer limited by this concentration. It allows the $NO_3$ to reach the expected values. The results are presented in Figure 2.7.

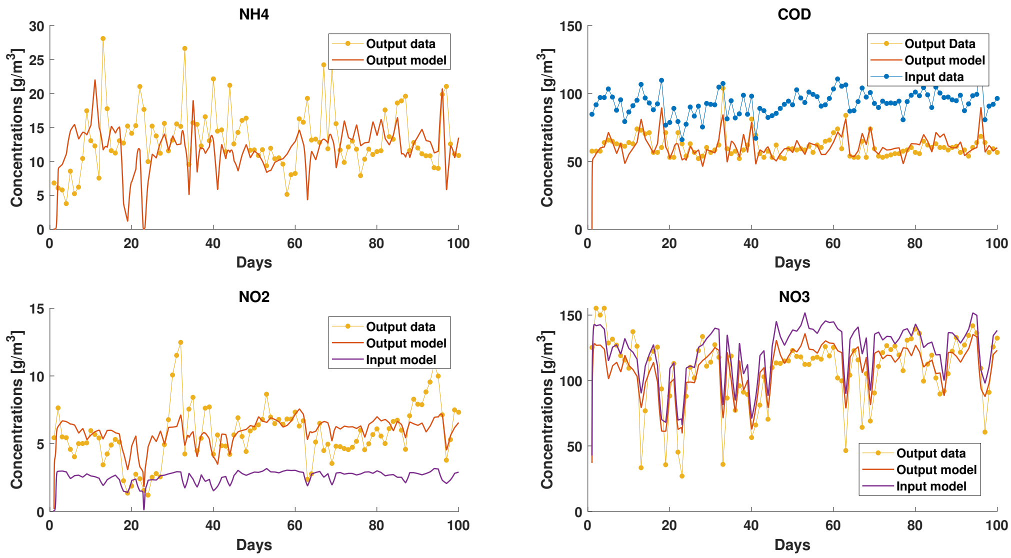


Figure 2.7: Input and output concentration of the simulation with new parameters for the post-denitrification stage in 2009

At first view, results looks satisfying since the model and the data output are the same order. Moreover, it should be noted that the model has difficulty predicting the $NH_4$ concentration and unexpected events such, e.g. the increases in $NO_2$ concentrations on day 30 and 95. In the following statistical analysis of the error is conducted. Figure 2.8 and 2.9 show the estimate probability distribution of the error for each concentration and the normalized error respectively.

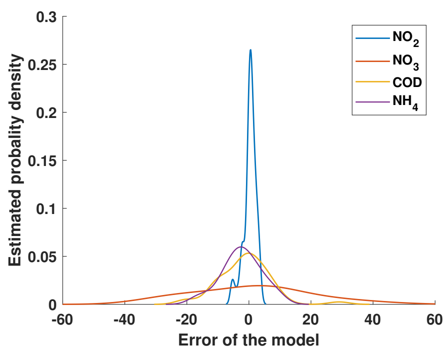


Figure 2.8: Estimate distribution of the model error

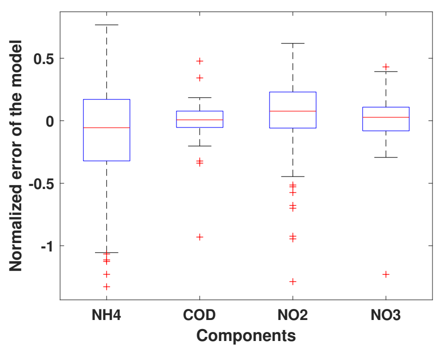


Figure 2.9: Boxplot of the normalized error for the different components

It can be seen on these two figures that the model error is centered close to zero (see ME in Table 2.10). The figure 2.9 allows to say that the error percentage is more concentrated around zero for the COD and the $NO_3$. The $NH_4$ has the normalized error the most dispersed. Table 2.10 present more precise information concerning the model error.

| | COD | $NH_4$ | $NO_2$ | $NO_3$ $[mg/L]$ |
|---|---|---|---|---|
| ME | 0.3 | -1.2 | 0.08 | 2.6 |
| Error std | 7.2 | 5.74 | 1.75 | 16.12 |
| MEA | 5.3 | 4.31 | 1.3 | 12.8 |
| MSE | 7.2 | 5.8 | 1.7 | 16.3 |
| $R^2$ | 0.13 | -0.73 | 0.31 | 0.62 |

Table 2.10: Statistical score results for the nitrification and post-denitrification stage simulation with new parameters in 2009

The factor $R^2$ is defined in Equation 2.8:

$$R^2 = 1 - \frac{\sum_{i=1}^{n} (y_i - \hat{y}_i)^2}{\sum_{i=1}^{n} (y_i - \bar{y})^2} \tag{2.8}$$

with $y_i$, $\hat{y}_i$, $\bar{y}$ the actual, expected and average output respectively.

This coefficient is as a ratio between the error made by the model and the error made by a simple model outputting only the average output value.

Given that, it can then be noticed that :

- COD : Despite the small error made by the model for COD, it does barely better than the average. This can be explained by the low variance of the output concentration in COD. Nevertheless one can see that the model allows to predict peak concentrations (see Figure 2.7).
- For $NO_3$ the model is much better than the average model.
- The model is also doing better for $NO_2$.
- The quality of the model for $NH_4$ is rather bad since it is not better than the average.

## 2.4 Pre-denitrification

In this section, the data available for the pre-denitrification section are presented. The pre-denitrification model has the same parameter problems as the post-denitrification since calibrated on the same dataset. New parameters for the model are therefore proposed based on the data and the re-calibrated parameters obtained for the post-denitrification model.

### 2.4.1 Data

The only representative data for this section are the average values of measurements taken on an equivalent plant, i.e. the Seine-Grésillons plant between 2015 and 2016. Its pre-denitrification biofilters are composed of 12 biostyr of 605 $m^3$. The values are provided in Table 2.11.

| | COD | $NO_2$ | $NO_3$ $[mg/L]$ | Q $[m3/s]$ |
|---|---|---|---|---|
| Data input | 82.5 | 1.84 | 32.2 | 3.68 |
| Data output | 39.26 | 0.85 | 18.7 | 3.68 |

Table 2.11: Mean I/O concentrations of pre-denetrification of SEG in 2015-16

### 2.4.2 New calibration

As no data are available for a complete calibration, it is decided to use a part of the calibrated parameters from the post-denitrification. Indeed, the reactions are identical. The two sections differ by their operating conditions and by the fixed medium where the bacteria develop (biostyr vs. biofor).

To fit correctly the model of this stage the yields coefficient $Y_9$,$Y_{10}$ and the concentration $X_4$ are adapted. As the data are mean values, these parameters can be find in an analytical way with the Equation system 2.11.

$$0 = \frac{Q_{\text{in}}}{V_{\text{post}}} \left([\text{COD}_{\text{in}}] - [\text{COD}_{\text{out}}]\right) - \frac{\mu_5}{Y_8} x_3 - \frac{\mu_6}{x_1} x_3 \tag{2.9}$$

$$0 = \frac{Q_{\text{in}}}{V_{\text{post}}} \left([\text{NO}_{2,\text{in}}] - [\text{NO}_{2,\text{out}}]\right) + \frac{\mu_5}{x_2} x_3 - \mu_6 x_3 \tag{2.10}$$

$$0 = \frac{Q_{\text{in}}}{V_{\text{post}}} \left([\text{NO}_{3,\text{in}}] - [\text{NO}_{3,\text{out}}]\right) - \mu_5 x_3 \tag{2.11}$$

$$\mu_5 = \mu_{5,\max} \frac{[\text{NO}_{3,\text{out}}]}{K_{\text{NO}_3,2} + [\text{NO}_{3,\text{out}}]} \frac{[\text{COD}_{\text{out}}]}{K_{\text{COD},3} + [\text{COD}_{\text{out}}]} = \text{cst} \tag{2.12}$$

$$\mu_6 = \mu_{6,\max} \frac{[\text{NO}_{2,\text{out}}]}{K_{\text{NO}_2,3} + [\text{NO}_{2,\text{out}}]} \frac{[\text{COD}_{\text{out}}]}{K_{\text{COD},4} + [\text{COD}_{\text{out}}]} = \text{cst} \tag{2.13}$$

**Results :** $x_2 = Y_{10} = 2.3 \qquad x_1 = Y_9 = 0.297 \qquad x_3 = X4 = 465.6\,[g/m^3]$

This calibration is to be taken with precaution given the small amount of information available. It will be necessary to re-calibrate the model on complete and recent measurements when they will be available.

## 2.5 Discussion and perspectives

In this section the results obtained will be discussed and some improvement for future work will be proposed.

### 2.5.1 Discussion

The tests performed showed that the initial implementation of the model did not successfully predict the observed concentration values.

With the few available data, a new calibration was proposed.This one allows the model to take into account dynamics previously omitted due to the initial values of the calibrated parameters. It also allows to restore coherent values with respect to the observed data. Nevertheless the calibration of the system remains approximate in view of the small amount of data available.

Two dynamics remain not considered by now. The one of oxygen to nitrification and the one from an external contribution in methanol in denitrification.
The first one is difficult to observed because the variation of oxygen is low. This is because the oxygen supply is carrefuly managed at the Seine-Aval.
The second was not considered so no data were available for the methanol flow.

### 2.5.2 Perspectives

To improve the quality of the model it is imperative to re-calibrate each block independently on data coming. If possible directly from the Seine-Aval WWTP. Furthermore, one should visit the site and work in closer collaboration with the SIAAP to have more precise informations on the operating conditions of the plant.

## Conclusion

This part started with the presentation of the implementation of the model. Then each block of the model were tested and calibrated until obtaining results fitting to available data.

# Chapter 3

# Optimization

The idea developed in this chapter is to test optimisation methods on the Seine-Aval model to make predective control of the flow between the different units. The final goal is to improve the quality of the water rejected in the Seine.

The advantage of optimization is to consider all the non-linear effects of the control variables. However the drawback is that the larger the number of control variables, the larger the required time for optimization. Therefore, there is a delay between measurements and control action.

In view of a possible real-world deployment, one wanted to test the robustness of the algorithm on three typical scenarios.

This chapter starts with the presentation of the chosen scenarios. Then, the optimization strategy is explained. Finally the optimization is applied on the chosen scenarios and the results are presented and commented.

## 3.1 Scenarios

The objective of the scenarios is to represent the operating conditions in case of dry day, normal rain and heavy rain. They consist in a fixed signal (concentrations & inlet flow) of one day duration. To design these scenarios the input data of the station between 2009 and 2014 are analyzed.

To help on this analysis, Figure 3.1 shows the distribution of the observed flow rate of the wastewater. As it can be seen, the flow distribution fit to a Inverse-Guaussian distribution. Such a distribution is explained by the contribution of rainfall and domestic wastewater to the flow.

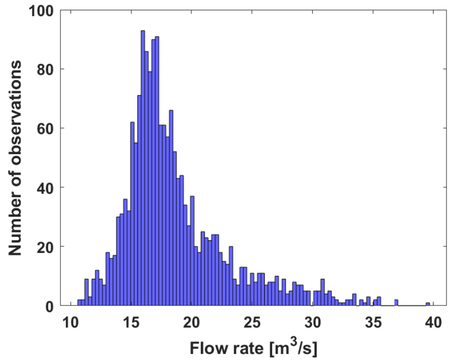


Figure 3.1: Distirbuton of the observed flow between 2009 and 2014 at the Seine-Aval wastewater treatment plant

The distribution of the observed concentrations are shown in Figure 3.2. It displays the distributions in case of normal, small and large flow for Normal Rain, Dry Day and Heavy Rain scenario respectively. Small and large flow are defined as the 5% of the smallest and largest observed flow respectively.

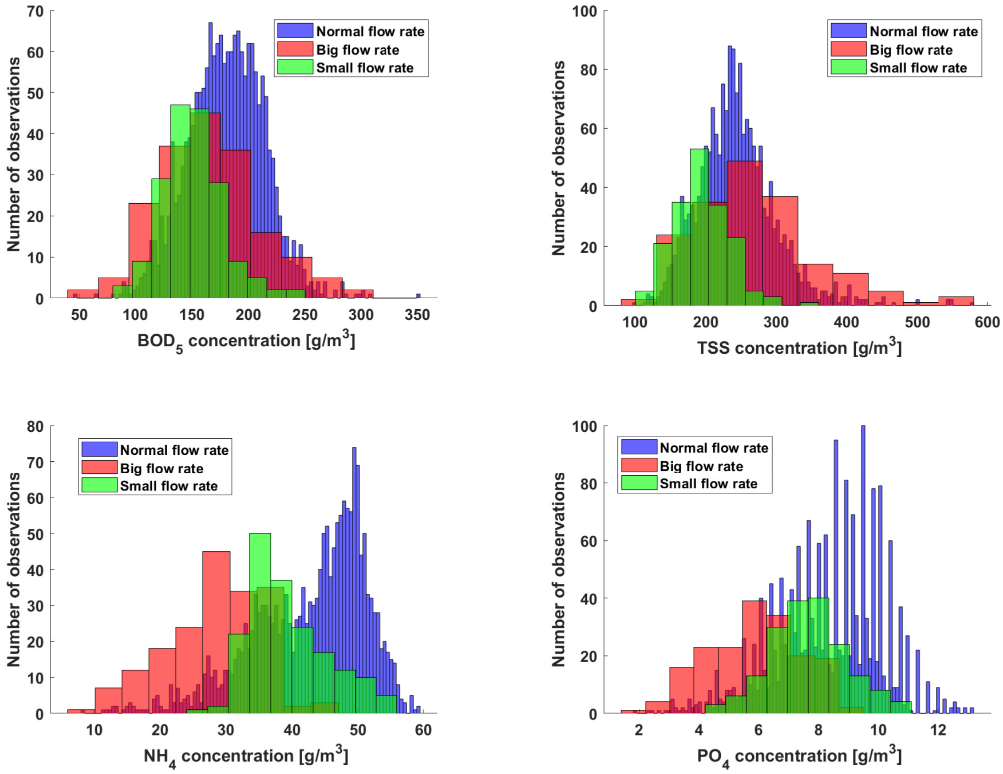


Figure 3.2: Distribution of the concentrations for normal, small and big flow rate at the input of Seine-Aval wastewater treatment plant between 2009 and 2014

A ratio of 2.5 is taken between COD and BOD. This ratio value comes the Jialu's thesis [13]. The results are shown on the Table 3.1.

| | TSS | $PO_4$ | COD | $NH_4$ | $NO_2$ | $NO_3$ $[mg/L]$ | Q $[m3/s]$ |
|---|---|---|---|---|---|---|---|
| Normal rain | 244.5 | 8.3 | 347.8 | 42.8 | 0.0 | 0.0 | 18.7 |
| Dry | 200 | 8.3 | 300 | 35 | 0.0 | 0.0 | 12 |
| Heavy rain | 244.5 | 6 | 347.8 | 28 | 0.0 | 0.0 | 28 |

Table 3.1: Concentrations and flow rate use for the scenario Rain, Dry and Heavy Rain

## 3.2 Initial conditions

The model is set in the standard configuration (i.e. a recirculation of 80 % and the bypass only used to respect the flow constraints) before any optimization. The concentrations and the inlet flow rates are given in the Table 3.2. Table 3.2 give the equilibrium concentrations obtained for all the basins.

| | | TSS | COD | $PO_4$ | $NH_4$ | $NO_2$ | $NO_3$ $[mg/L]$ | Q $[m3/s]$ |
|---|---|---|---|---|---|---|---|---|
| Input | Rain scenario | 244.5 | 347.8 | 8.3 | 42.8 | 0.0 | 0.0 | 18.7 |
| | First settler | 39.64 | 139.93 | 6.76 | 42.8 | 0.0 | 0.0 | 18.7 |
| | Pre-denitrification | 39.64 | 74.27 | 6.76 | 26.77 | 1.19 | 38.7 | 31.25 |
| Equilibrium | Nitrification | 39.64 | 78.97 | 6.76 | 9.3 | 3.1 | 106.02 | 33.66 |
| | Post-denitrification | 39.64 | 12.18 | 6.76 | 9.3 | 3.53 | 89.36 | 11.5 |
| | Second settler | 6.08 | 15.05 | 4.91 | 9.3 | 3.35 | 96.04 | 18.7 |

Table 3.2: Equilibrium concentrations of the model of the Seine-Aval wastewater treatment plant for Normal scenario with usual flow management

## 3.3 Optimisation presentation

This section starts by outlining the constraints on the control variables. Then it explains different ways of calculating the objective function and the different optimisation strategies.

### 3.3.1 Constraint

The physical constraints corresponding to the various flow limits of the different unit of the Seine-Aval wastewater are shown in the following Equations. For a better understanding see Figure 1.1 presented in the section 2.1.

$$0 \leq u_r \leq 16 m^3/s$$

$$Q + u_r \leq 50.40\, m^3/s \qquad 0 \leq u_{1,b} \leq Q m^3/s \qquad \sum_{i=1}^{3} u_{p,i} = Q + u_r - u_b$$

$$Q + u_r - u_{1,b} \leq 31.25\, m^3/s \qquad 0 \leq u_{p,i} \leq 10.42 m^3/s \qquad \sum_{i=1}^{6} u_{n,i} = Q + u_r$$

$$0 \leq u_{n,j} \leq 8.4 m^3/s$$

### 3.3.2 Objective function and strategy

The objective function used is the Effluent Quality Index (EQI) defined in previous section 1.3.3. As a reminder, EQI is a weighted sum of the polluant outputs. Therefore, the model needs to be run to calculate the pollutant concentration. These concentration are a function of the control variables and the scenario. Three optimization strategies have been investigated :

- The first is to optimize the EQI according to the recirculation ($u_r$) and denitrification bypass ($u_{b,1}$).

$$\mathrm{EQI}_1 = f(u_{b,1}, u_r) \tag{3.1}$$

- The second strategy consists in optimizing according to all the flows that can be controlled (11 in total).

$$\mathrm{EQI}_2 = f(u_{b,1}, u_r, u_{p,i}, u_{n,j}) \tag{3.2}$$

- The last is to optimize according to the number of denitrification basins $N_{pre}$ and nitrification basins $N_{nitri}$ open (zero flow for the other basins) as well as according to $u_r$ and $u_{b,1}$.

$$\mathrm{EQI}_3 = f(u_{b,1}, u_r, N_{\mathrm{pre}}, N_{\mathrm{nitri}}) \tag{3.3}$$

The algorithms used are SQP and Genetic Algorithm for $\mathrm{EQI}_1$ and $\mathrm{EQI}_2$. Only the Genetic Algorithm is used for $\mathrm{EQI}_3$ since it deals with the discrete values $N_{\mathrm{pre}}$ and $N_{\mathrm{nitri}}$.

## 3.4 Results

Concerning the optimization of $EQI_2$ and $EQI_3$, the modification of the distribution of the flows $u_{p,i}$ and $n_{p,j}$ showed no improvement in objective function. The results shown in this section are therefore the analysis of the behavior of $EQI_1$, i.e. the objective function with respect to the variation of the recirculation and bypass flows. The optimization is studied for each of the three scenarios.The reader is invited to look at the diagram 1.1 of treatment plants in the Section 1.2 to better understand the explanations given.

### 3.4.1 Normal Rainy Day

As it can be seen in the Figure 3.3, the optimal flow configuration for the normal rain scenario is to take the largest possible recirculation, i.e. the maximal flow before the requirement of the denitrification bypass.

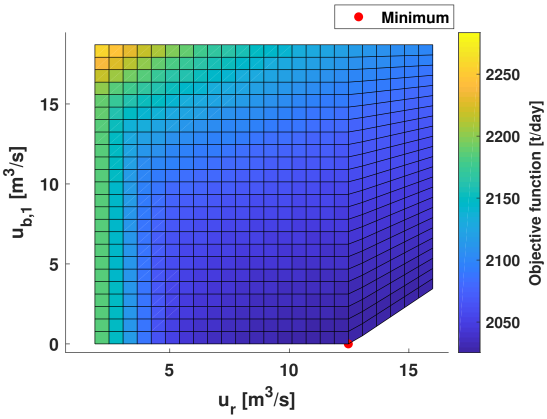


Figure 3.3: Objective function in function of the pre-denitrification bypass and recirculation flow rate for Normal scenario

Table 3.3 gives the information about the efficiency of the algorithms to find the optimum. One observes that the SQP algorithm is faster than the Genetic algorithm to find the optimum. Moreover the genetic algorithm needs to be tuned correctly to find the optimum which makes it more difficult to use. The tuning strategy is to fix the population size at 40 and to allow a maximum of 3 generations.

| Algorithm | Iterations | Function eval. | Time [s] | Constraint |
|---|---|---|---|---|
| SQP | 34 | 105 | 50.9 | OK |
| GA | 3 | 160 | 81 | OK |

Table 3.3: Results of the SQP and GA algorithm to find the optimum $u_r$ and $u_b$ for Normal day scenario

The objective function in this optimization is mainly a function of the quantity of nitrogen in the treated water. Figure 3.5 and 3.4 show the objective function depending on the flow variations and the consumption of nitrogen in the denitrification and post-denitrification sections.

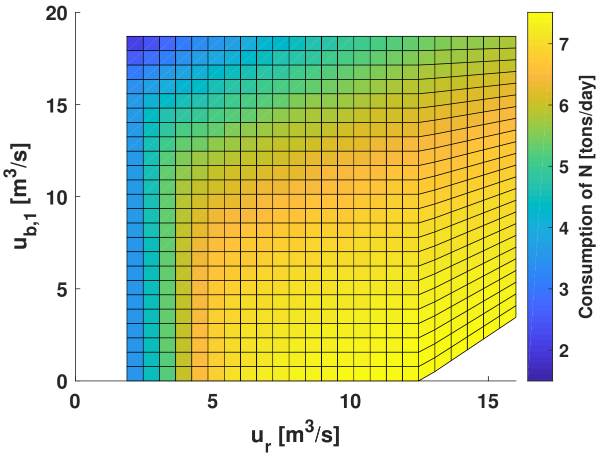


Figure 3.4: Consumption of N at the pre-denitrification for Normal scenario

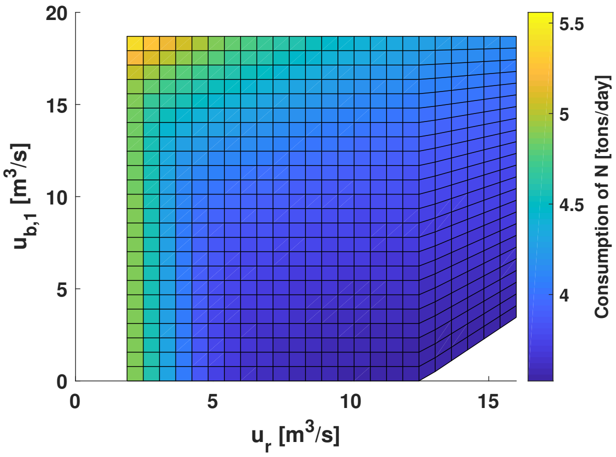


Figure 3.5: Consumption of N at the post-denitrification for Normal scenario

Figure 3.4 shows that the consumption of N in the pre-denitrification stage increases with the recirculation flow rate. This increase is large at the beginning and decreases more and more with higher recirculation flow. The Figure also highlights that the bypass flow decreases the consumption of N at pre-denitrification stage for small recirculation flow.

Figure 3.5 shows that for the nitrogen consumption at the post denitrification stage has an antagonist behavior than at the pre-denitrification stage. It can also be observed that the variation is of a smaller range for the post-denitrification stage. As a result, the total consumption of N increases with the recirculation and decrease with the bypass flow rate.

The increase of the consumption of N with recirculation is becauce it is the only source of N for the pre-denitrification stage. Then, without recirculation the pre-denitrification is impactless to improve the treatment of N.

The decrease of the consumption of with the bypass of the pre-denitrification stage is more complex. In order to have a better view, Figure 3.6 shows a simulation of the plant while varying the bypass. It presents the results for the flow strategies $u_r = 5$ and $u_b = 0$ (case 1) and $u_r = 5$ and $u_b = 15$ (case 2).

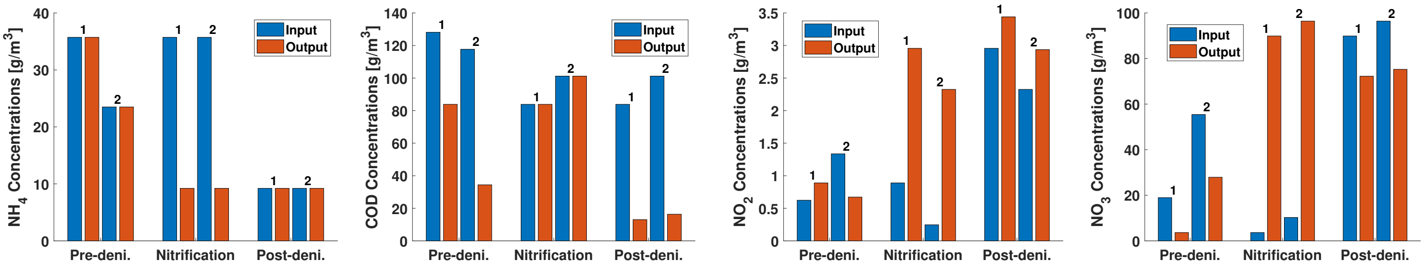


Figure 3.6: Concentrations at input and output of the different stages for normal rain simulation. Case 1: $u_b = 0$ and $u_r = 5$. Case 2: $u_b = 15$ and $u_r = 5$

In one hand, one can observe that the equilibrium concentrations of $NO_2^-$ and $NO_3^-$ in the pre-denitrification stage keep a value that do not affect the growth of bacteria (see $K_{NO_2}$ and $K_{NO_3}$). On the other hand, the lower carbon input (implied by the bypass $u_b = 15$) reduces the equilibrium concentration of COD that limits the growth of bacteria (see $K_{COD}$). To sum up, the consumption of N is limited by the carbon supply at the pre-denitrification.

One can also notice that a lower consumption in the pre-denitrification implies a higher flow of carbon at post-denitrification (e.g. case 2) and vice-versa (e.g. case 1). For case 2, this results in a higher concentration of carbon at output/equilibrium in the post-denitrification. This can be observed in Figure 3.6 where case 2 has a higher carbon concentration than case 1. Even if difference looks small, the COD concentrations is in a range that has a noticeable effect on the consumption of N. The consumption of N for case 1 and 2 is given in the Figure 3.7.

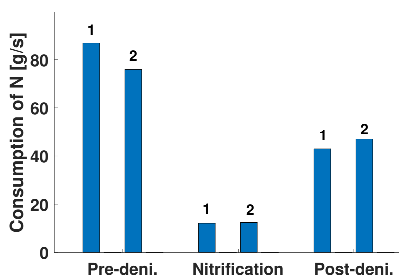


Figure 3.7: Consumption of N in [g/s] at the different stage of the wastewater treatment plant. Case 1: $u_b = 0$ and $u_r = 5$ Case 2: $u_b = 15$ and $u_r = 5$

### 3.4.2 Dry day

Figure 3.8 shows that the optimal flow configuration for dry weather scenario is to take the largest possible recirculation flow with no bypass flow rate.

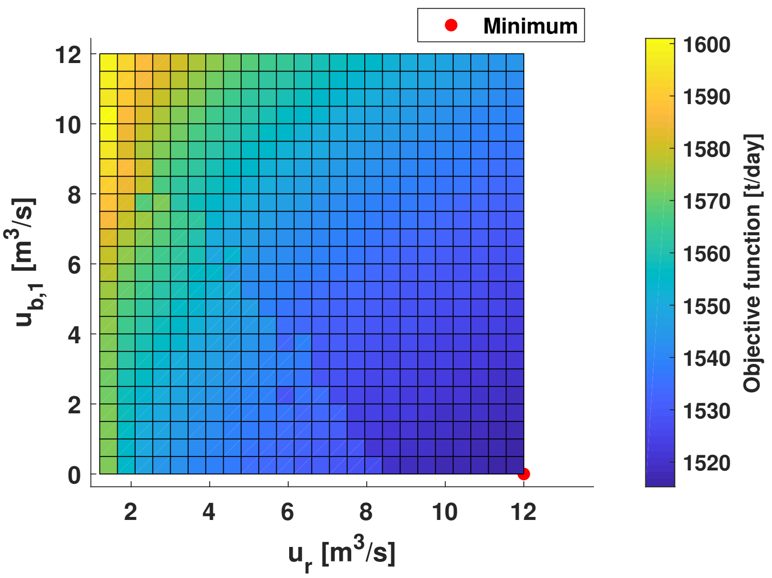


Figure 3.8: Objective function in function of the pre-denitrification bypass and recirculation flow rate for Dry scenario

Table 3.4 gives the information about the efficiency of the algorithms to find the optimum. One observes that the SQP algorithm and the Genetic Algorithm have the same range of time to find the optimum.

| Algorithm | Iteration | Function eval. | Time [s] | Constraint |
|---|---|---|---|---|
| SQP | 34 | 182 | 92 | OK |
| GA | 3 | 160 | 94 | OK |

Table 3.4: Results of the SQP and GA algorithm to find the optimum $u_r$ and $u_b$ for Dry day scenario

Figure 3.9 and 3.10 shown the consumption of N at the pre-denitrification stage and at the post-denetrification stage.

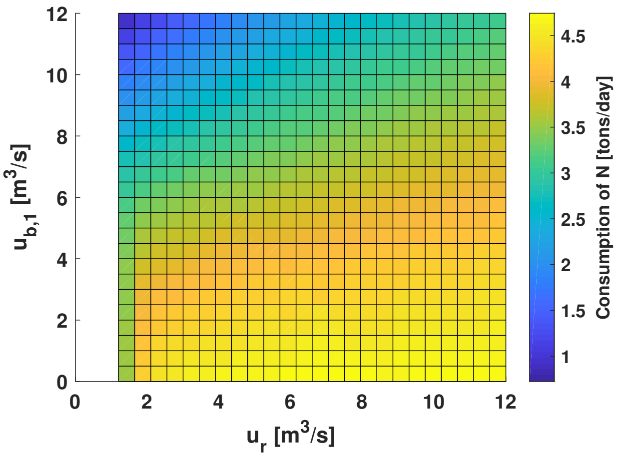


Figure 3.9: Consumption of N at the pre-denitrification for Dry scenario

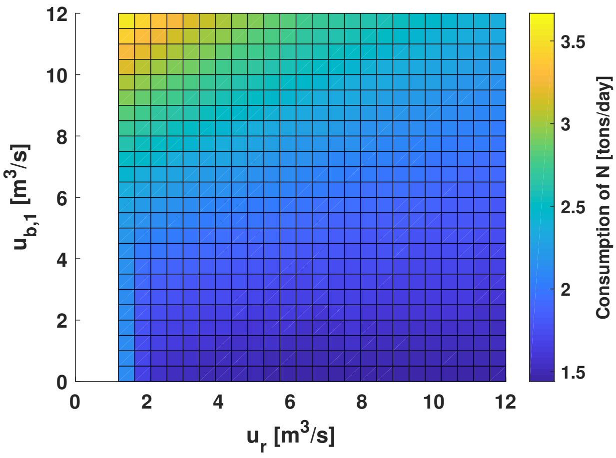


Figure 3.10: Consumption of N at the post-denitrification for Dry scenario

It is noticeable that the consumption of N is less dependent on the recirculation flow and is more sensitive to the bypass flow. To better understand the mechanisms, it is interesting to study the impact of the flows $u_r$ and $u_b$ variations on the concentrations. An example of the data studied is available in Appendix. Based on those test, conclusions can be drawn.

Given the low flow rate at the nitrification stage, all of the $NH_4$ is consumed. Thus it produce a lot of nitrite and nitrates. The recirculation flow is therefore very concentrated in nitrite and nitrates. Since the inlet flow rate of the WWTP is low, the mix with the recirculation results in a flow with a high concentration of nitrites and nitrates.

To sum up, in one hand, given that the concentrations of nitrates and nitrites are high, their increase is not decisive in the dynamics of the denitrification stage. On the other hand, the COD concentrations and mass flow rate become the key parameter. That explains the importance of not bypassing the pre-denitrification stage so that provide enough carbon to promote the consumption of nitrites and nitrates. By the same reasoning, the increase of the bypass results in more carbon for the post-denetrification stage and so, a bigger consumption of N.

### 3.4.3 Heavy rain

Figure 3.11 shows that the optimal flow configuration for the haevy rain scenario is to take the largest possible recirculation flow and no bypassing flow rate. Contrary to the normal rain scenario, it seems more beneficial to increase the recirculation. It bring advantages, even when it is necessary to increase the bypass $u_b$ due to the flow limits of the denitrification stage.

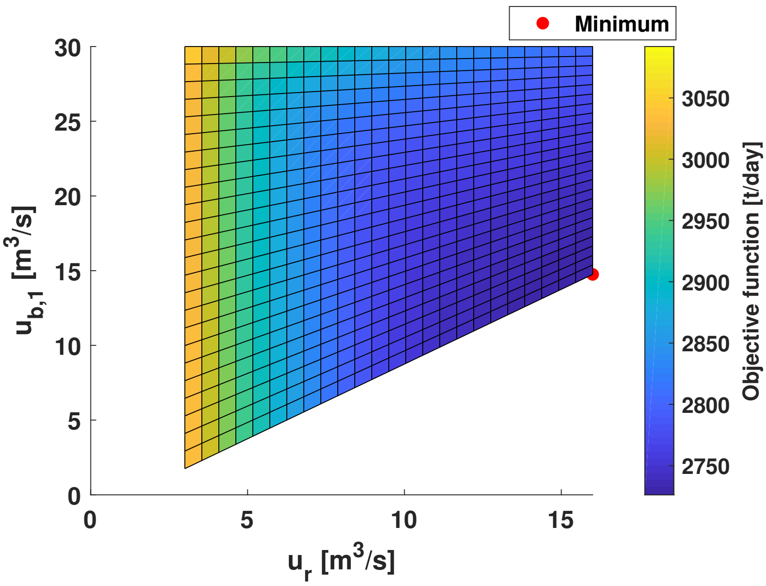


Figure 3.11: Objective function in function of the pre-denitrification bypass and recirculation flow rate for Rain scenario

Table 3.3 gives the information about the efficiency of the algorithms to find the optimum. One observes that the SQP algorithm is faster than the Genetic algorithm to find the optimum.

| Algorithm | number of iteration | Function eval. | Time [s] | Constraint |
|---|---|---|---|---|
| SQP | 34 | 105 | 50 | OK |
| GA | 3 | 160 | 99.4 | OK |

Table 3.5: Results of the SQP and GA algorithm to find the optimum $u_r$ and $u_b$ for Heavy rain scenario

Figures 3.12 and 3.13 show that, compared to the other scenarios, the consumption variations is more dependant to recirculation and less to the bypass

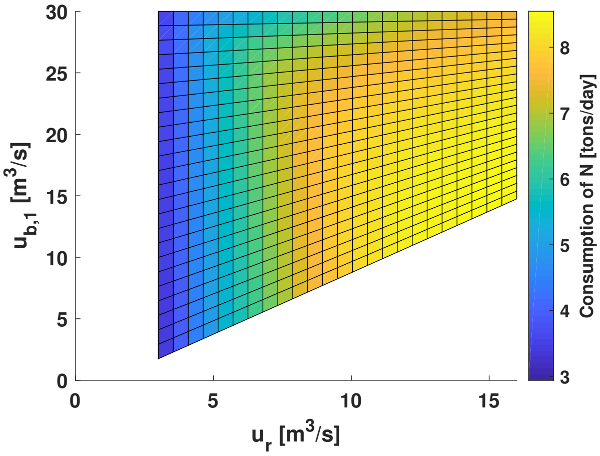


Figure 3.12: Consumption of N at the pre-denitrification during Heavy Rain

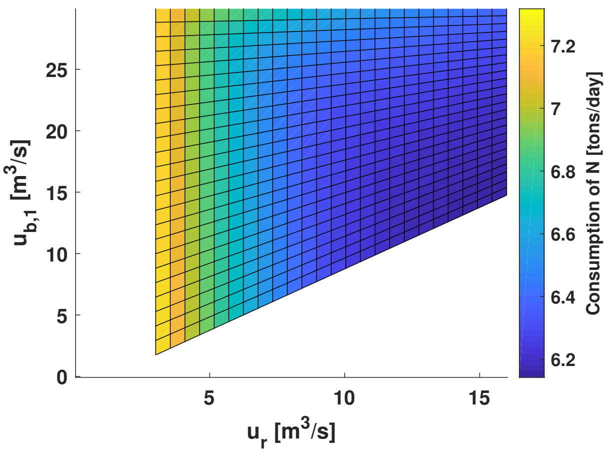


Figure 3.13: Consumption of N at the pre-denitrification during Heavy Rain

To give a better understanding, station was simulated for the following two cases: case 1 $u_b = 2$ & $u_r = 16$ and case 2 $u_b = 2$ & $u_r = 2$. The concentrations obtained at the different sections of the station are available in Figure 3.14.

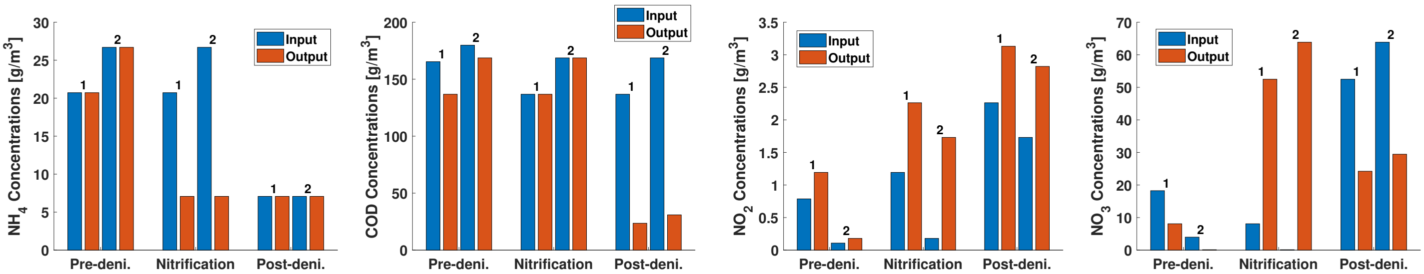


Figure 3.14: Concentrations at input and output of the different stages for heavy rain simulation . Case 1: $u_b = 2$ and $u_r = 16$. Case 2: $u_b = 2$ and $u_r = 2$

Contrary to the other scenario, Figure 3.14 shows that it is no longer the equilibrium concentration of COD that is limits the pre-denitrification (see $K_{\mathrm{COD}}$). Actually, this concentration stay high even with a higher recirculation flow. Then, one observe that the limiting factors are the equilibrium concentrations of $NO_2^-$ and $NO_3^-$. Indeed, the equilibrium concentrations of $NO_2^-$ and $NO_3^-$ reach a very low values when the recirculation flow is low.

## 3.5 Discussion and perspectives

To bring a critical look at the results shown, here is a discussion. Also, perspectives and improvements are presented.

### Discussion

Some control variables are impactless on the objective function. Therefore, it was not possible to test the robustness and efficiency of the algorithms for a large number of variables.

Nevertheless, it was possible to show the results of the optimisation of two control variables ($u_r$ and $u_b$). An analysis of these showed the importance of having an adapted management of the flows. This, to maintain the equilibrium concentrations of COD, $NO_2^-$ and $NO_3^-$ in sufficient values in the pre-denitrification unit. That allows efficient consumption of nitrogen.

Moreover, without the complexificaiton of the model and without a calibration on actual data, these results remain only a first steps towards the study of the control of flows.

### Perspectives

In future work, it would be interesting to :

- Study the use of such algorithms for more complete models taking into account additional control variables such as metanol or oxygen supply.
- Complement the objective function by integrating for example the minimisation of sludge production, operating costs and/or energy consumed by the pumps[33].
- Consider multi-objective optimisation methods as in the work of Berau et al. [34] .

# Conclusion

This section has presented three scenarios representing three typical conditions of WWTP operations. Then different strategies to optimize the control variables for these scenarios were described. Genetic Algorithm and the Sequential Quadratic Program have been tested on these strategies. The results obtained for this optimization have been developed and finally discussed.

# Conclusion

This master thesis explained the implemention a model of the Seine-Aval wastewater treatment plant and propose a control strategy to improve the quality of the water discharged into the Seine. The possibility to perform predictive control via optimization algorithms has been studied. It consisted in testing this strategy for three typical operating conditions of the station : dry weather, normal rain and heavy rain.

In order to achieve this objective, it was first necessary to study the state of the art related to wastewater treatment. For this purpose, the composition of the wastewater and the legislation of the WWTP were detailed. After that a brief explanation of the main steps of wastewater treatment was given. Following this, a detailed description of the infrastructure and operating conditions of the Seine-Aval plant was made. Then, the models used to simulate the different sections have been developed. Finally, the theoretical basis for the formulation of an optimization problem and the algorithms that can be used were presented.

In a second step, the models of each section of the WWTP were developed based on the work done by Ben Ayed et al. After their implementation, each model were tested on the corresponding available data. The results of these tests were not conclusive so the models were re-calibrated and get better. This work of analysis of the model quality and recalibration was an important part of this thesis.

Finally, the optimization of the flows between the different sections was proposed in order to reach a better quality of water rejected in the Seine. To prove the robstness of the optimization, it was applied on three different scenarios : normal rain, dry weather and heavy rain. These three operating conditions have been developed based on the available daily data. Then, the results were presented and discussed.

The optimizations exposed good results in a reasonable amount of time.

The **contributions** of this work were:

- The implementation of a model of the Seine-Aval WWTP in the Simulink interface of Matlab. It allows an easy-use and modification of the model. The code is available on Github.
- An analysis and recalibration of this model.
- The development of a framework to test different optimization methods on the model.
- The in-depth study of the results of the optimization of flows between basins for three typical scenarios.

The **next steps** are :

- An implementation of these optimization techniques in the framework of non-linear predictive control.
- The calibration of the model with current data from the treatment plant.
- The complexification of the model by taking into account the methanol contribution
- The study of an optimization of more parameters such as energy costs, economic operation of the plant or the production of sludge.

# Bibliography

[1] European Commission, "Nouvelle enquête Eurobaromètre: Protéger l'environnement et le climat est important pour plus de 90% des citoyens européens," 2020. [Online; accessed 06-April-2022].

[2] Council of the European Union, "Council Directive 91/271/EEC of 21 May 1991 concerning urban waste-water treatment," 1991. [Online; accessed 06-April-2022].

[3] European Commission, "Urban Waste Water Treatment Directive - Review," 2019. [Online; accessed 06-April-2022].

[4] European Commission, "Revision of the Urban Waste Water Treatment Directive (Ref. Ares(2020)3769112)," 2020. [Online; accessed 06-April-2022].

[5] A. B. Ayed, D. Dochain, I. Prodan, and C. E. Robles-Rodriguez, "Centralized model predictive control of the wastewater treatment plant of seine-aval," in *2021 25th International Conference on System Theory, Control and Computing (ICSTCC)*, pp. 643–648, IEEE, 2021.

[6] M. Henze and Y. Comeau, "Wastewater characterization," *Biological wastewater treatment: Principles modelling and design*, pp. 33–52, 2008.

[7] SIAAP, "DÉPOLLUER LES EAUX USÉES," /. [Online; accessed 16-May-2022].

[8] C. Eme and C. Boutin, "Composition des eaux usées domestiques par source d'émission à l'échelle de l'habitation," *Publication Onema*, 2015.

[9] , "Arrêté du 21 juillet 2015 relatif aux systèmes d'assainissement collectif et aux installations d'assainissement non collectif, à l'exception des installations d'assainissement non collectif recevant une charge brute de pollution organique inférieure ou égale à 1,2 kg/j de DBO5," /. [Online; accessed 16-May-2022].

[10] EUR-Lex, "Commission directive 98/15/ec of 27 february 1998 amending council directive 91/271/eec with respect to certain requirements established in annex i thereof," *Official Journal of the European Communities*, vol. 67, pp. 29–30, 1998.

[11] V. V. Ranade and V. M. Bhandari, *Industrial wastewater treatment, recycling and reuse*. Butterworth-Heinemann, 2014.

[12] R. M. Stuetz and T. Stephenson, *Principles of water and wastewater treatment processes*. Iwa Publishing, 2009.

[13] J. Zhu, *Modélisation détaillée du fonctionnement de la future filière complète de biofiltration de la station de traitement des eaux usées Seine Aval*. PhD thesis, Université de Technologie de Compiègne, 2020.

[14] G. Bastin, *On-line estimation and adaptive control of bioreactors*, vol. 1. Elsevier, 2013.

[15] M. Henze, W. Gujer, T. Mino, T. Matsuo, M. C. Wentzel, G. v. R. Marais, and M. C. Van Loosdrecht, "Activated sludge model no. 2d, asm2d," *Water science and technology*, vol. 39, no. 1, pp. 165–182, 1999.

[16] J. B. . S. G. . S. Azimi, "Calibration et validation d'un modèle de décantation physico-chimique à l'échelle industrielle, le modèle simdec," *Eau, l'industrie, les nuisances*, vol. 391, no. 1, pp. 98–105, 2016.

[17] C. Robles-Rodriguez, J. Bernier, V. Rocher, and D. Dochain, "A simple model of wastewater treatment plants for managing the quality of the seine river," *IFAC-PapersOnLine*, vol. 51, no. 18, pp. 880–885, 2018.

[18] V. Rocher, C. Join, S. Mottelet, J. Bernier, S. Rechdaoui-Guérin, S. Azimi, P. Lessard, A. Pauss, and M. Fliess, "La production de nitrites lors de la dénitrification des eaux usées par biofiltration-stratégie de contrôle et de réduction des concentrations résiduelles," *Revue des sciences de l'eau/Journal of water science*, vol. 31, no. 1, pp. 61–73, 2018.

[19] Wikipedia contributors, "Nitrifying bacteria — Wikipedia, the free encyclopedia." `https://en.wikipedia.org/w/index.php?title=Nitrifying_bacteria&oldid=1085017431`, 2022. [Online; accessed 9-May-2022].

[20] M. A. Van Kessel, D. R. Speth, M. Albertsen, P. H. Nielsen, H. J. Op den Camp, B. Kartal, M. S. Jetten, and S. Lücker, "Complete nitrification by a single microorganism," *Nature*, vol. 528, no. 7583, pp. 555–559, 2015.

[21] J. Nocedal and S. J. Wright, *Numerical optimization.* Springer, 1999.

[22] M. E. Boomgaard, J. G. Langeveld, and F. H. Clemens, "Wastewater system optimisation using genetic algorithms," in *Urban Drainage Modeling*, pp. 788–796, 2001.

[23] C. Benthack, B. Srinivasan, and D. Bonvin, "An optimal operating strategy for fixed-bed bioreactors used in wastewater treatment," *Biotechnology and bioengineering*, vol. 72, no. 1, pp. 34–40, 2001.

[24] M. Mitchell, *An introduction to genetic algorithms.* MIT press, 1998.

[25] The MathWorks, Inc., "How the genetic algorithm works." `https://www.mathworks.com/help/gads/how-the-genetic-algorithm-works.html#f13721`, 2022. [Online; accessed 2-May-2022].

[26] MATLAB, *version 9.4.0 (R2018b).* Natick, Massachusetts: The MathWorks Inc., 2018b.

[27] P. A. Vanrolleghem, U. Jeppsson, J. Carstensen, B. Carlssont, and G. Olsson, "Integration of wastewater treatment plant design and operation—a systematic approach using cost functions," *Water Science and Technology*, vol. 34, no. 3-4, pp. 159–171, 1996.

[28] Y. Amerlinck, S. Gillot, and P. A. Vanrolleghem, "Benchmarking wwtp control strategies with robustness and economic measures as performance criteria," in *Proc. Water Environ. Fed. 74th Annu. Conf. Exposition [CD-ROM], Atlanta, Ga*, 2001.

[29] J. Guerrero, A. Guisasola, R. Vilanova, and J. A. Baeza, "Improving the performance of a wwtp control system by model-based setpoint optimisation," *Environmental Modelling & Software*, vol. 26, no. 4, pp. 492–497, 2011.

[30] M. F. Nezhad, N. Mehrdadi, and A. Torabian, "Definition of a new domestic effluent quality index using topsis decision making tool," *Canadian Journal of Pure and Applied Sciences*, vol. 9, no. 2, pp. 3467–3472, 2015.

[31] I. Nopens, L. Benedetti, U. Jeppsson, M.-N. Pons, J. Alex, J. B. Copp, K. V. Gernaey, C. Rosen, J.-P. Steyer, and P. A. Vanrolleghem, "Benchmark simulation model no 2: finalisation of plant layout and default control strategy," *Water Science and Technology*, vol. 62, no. 9, pp. 1967–1974, 2010.

[32] SIAAP, "Fiches usines : Usine d'épuration Seine aval," tech. rep., 2013.

[33] E. Tejaswini, S. Panjwani, U. B. B. Gara, and S. R. Ambati, “Multi-objective optimization based controller design for improved wastewater treatment plant operation,” *Environmental Technology & Innovation*, vol. 23, p. 101591, 2021.

[34] B. Béraud, J.-P. Steyer, C. Lemoine, E. Latrille, G. Manic, and C. Printemps-Vacquier, “Towards a global multi objective optimization of wastewater treatment plant based on modeling and genetic algorithms,” *Water science and technology*, vol. 56, no. 9, pp. 109–116, 2007.

# A Results for validation period

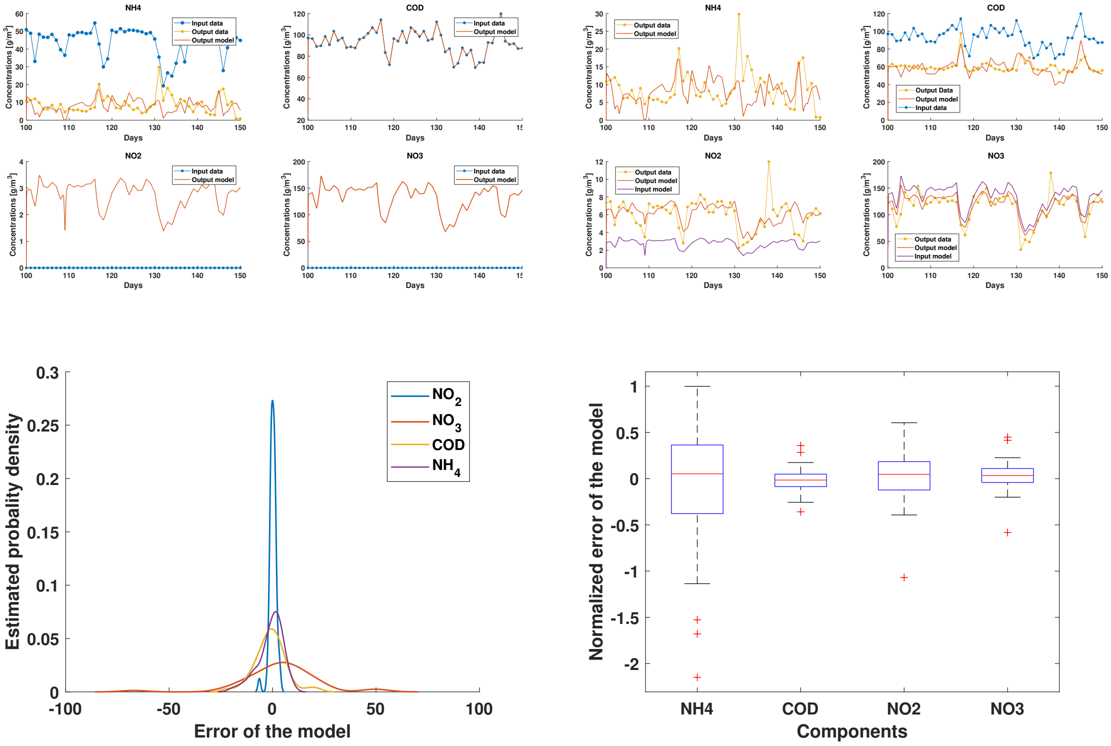


Figure 15: Results for the nitrification and post-denitrification stage simulation for the validation period

# B Dry weather example

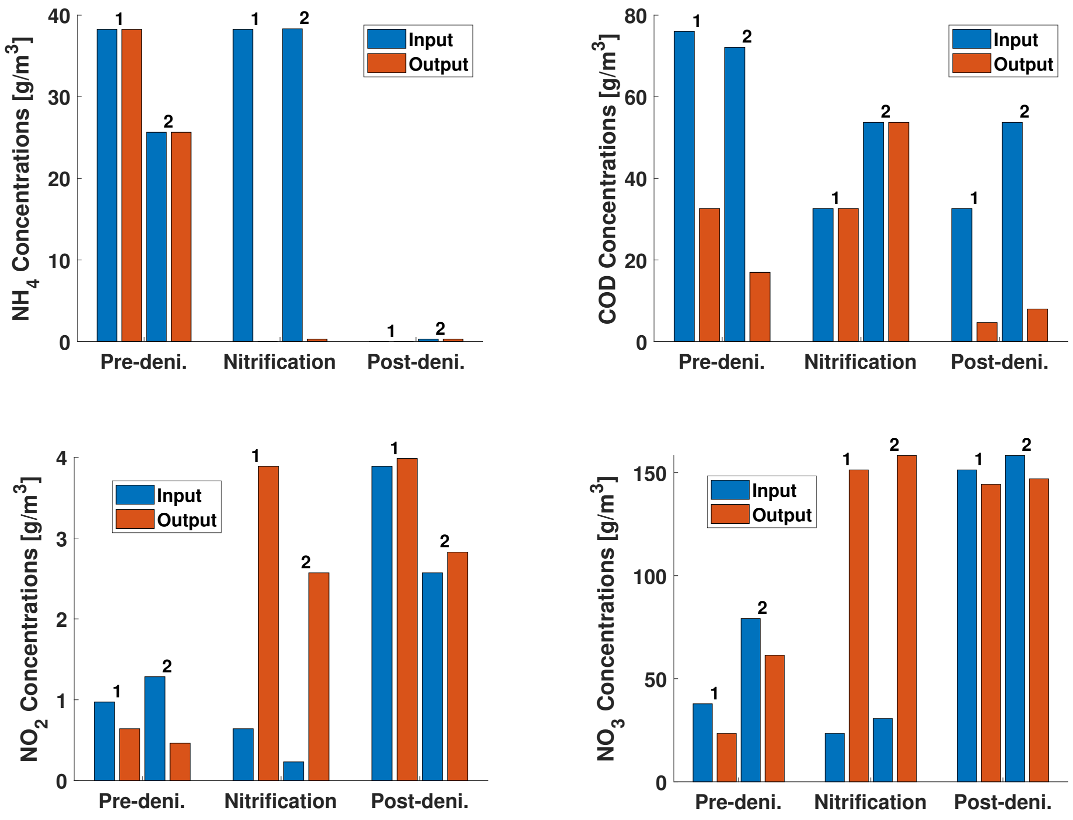


Figure 16: Concentrations at input and output of the different stages for dry scenario . Case 1: $u_b = 0$ and $u_r = 4$ Case 2: $u_b = 8$ and $u_r = 4$

**UNIVERSITÉ CATHOLIQUE DE LOUVAIN**
**École polytechnique de Louvain**
Rue Archimède, 1 bte L6.11.01, 1348 Louvain-la-Neuve, Belgique | **www.uclouvain.be/epl**